



UNIVERSITAT DE
BARCELONA

Facultat de Matemàtiques
i Informàtica

GRAU DE MATEMÀTIQUES

Treball final de grau

Surface Visualization via Level Curves and Applications

Autora: Neus Herranz Lozano

Director: Dr. Antoni Benseny Ardiaca

Realitzat a: Departament de Matemàtiques i Informàtica

Barcelona, 21 de juny de 2020

Contents

Abstract	iii
Project structure	iii
Acknowledgements	iii
1 Introduction to surface visualization	1
1.1 Surface levels	1
1.2 A simple example	2
2 Analytic study for surface representation	5
2.1 Level curves differential equation systems	5
2.2 Critical points and equilibrium: stability classification	6
2.3 Level curves	8
2.3.1 Level curves preparation	8
2.3.2 Level curves computation	10
2.4 Slices preparation	10
3 Program implementation	13
3.1 Trace for slicing	13
3.2 Bifurcation diagram	15
3.3 Curves and slices display	18
3.4 Simulation	18
3.5 Program organization	18
4 Global representation of the zero-velocity curves in the XPCR3BP	21
4.1 The extended two body problem	22
4.2 The extended potentials and their circular orbits	23
4.3 The extended planar and circular three-body problem	24
4.4 The XPCR3BP in non-dimensional units	25
4.5 Hamiltonian formulation of the XPCR3P in sinodic coordinates	27

4.6	Equilibrium points of the extended problem	27
4.6.1	Equilibrium points classification	28
4.7	Extended Jacobi constants and zero-velocity curves	29
4.8	Analysis of $\Omega_{\alpha,m}$ function	30
4.8.1	Characteristic points of $\Omega_{\alpha,m}$	31
4.8.2	Collision points	31
4.8.3	Equilateral equilibrium points	33
4.8.4	Collinear equilibrium points	34
4.8.5	Coincidences of extended Jacobi constants	35
4.8.6	Extended Jacobi constants ordering	37
4.8.7	Bifurcation diagrams of the extended Jacobi function	39
4.9	Bifurcation diagrams implementation	41
4.10	Surface visualization of zero-velocity curves	43
5	Results and conclusions	45
5.1	Results	45
5.1.1	Simulator	45
5.1.2	Surfaces depending on the α interval	47
5.2	Conclusions	48
A	The classical problem	51
A	Classical problem Jacobi constants	51
B	Zero-velocity curves description for the classical problem	52
C	Program code for the case $\alpha < -1$	52
B	Resulting images	57
	Bibliography	69

Abstract

This study intends to implement a 3-D surface representation via level curves. This way of representing surfaces requires a lot of previous work. Nevertheless, it is very useful when dealing with problems where it is important to know the points of the surface that are in each level cut.

A general simulator has been implemented in order to be easily adapted to different problems. The program code has been structured in a way in which it can be used for different surfaces. The simulator has been applied to the representation of zero-velocity curves of the extended planar and circular restricted 3-body problem (XPCR3BP).

This project aims to be as general as possible. However, some simplifications of the surface visualization via level curves problem have been taken into consideration in order to ease the programming purposes: the problem has been implemented only for simple closed curves; and the singular level curves associated to saddle points have been considered to be homoclinic.

Project structure

This document has been structured in five chapters. In chapter 1 the problem of surface representation via level curves is introduced along with a simple example is given. In chapter 2 the mathematical background related to surface representation via level curves is detailed. In chapter 3 some programming and implementation steps of the code are explained. In chapter 4 the extended planar and circular restricted 3-body problem is introduced. The aim of this chapter is to give the necessary information related to this specific problem in order to give an application for the visualization computation. Finally, in chapter 5, the results and conclusions of this work are presented and discussed.

Acknowledgements

I would like to thank my family and friends for all the support and love during the process of writing this project.

I would also like to acknowledge the help received by the local log association, my university friends and Josie. These university years would have not been the same without them.

Finally, I would specially like to thank Dr. Antoni Benseny Ardiaca for helping me during this process, for all the given advice and for his time and dedication.

Chapter 1

Introduction to surface visualization

1.1 Surface levels

Given a function $F : \mathbb{R}^2 \rightarrow \mathbb{R}$, the representation of the 3D surface associated to $z = F(x, y)$ can be approached in several different ways.

Firstly, the most intuitive method to display a 3D surface will be introduced. A 2D Cartesian mesh is taken in the space of (x, y) . The function, $F(x, y)$, is evaluated at the points of the mesh. The result is a 3D mesh plot in the space (x, y, z) .

The main aim of this work is to plot a surface but also to clearly display the level sets associated to the surface. If the surface is plotted by using the mesh technique, some features of contour plots can be used in order to display surfaces. However, these tools do not give a clear and precise display of their level sets.

Another way of solving this problem is by considering the reverse problem where the expression

$$z = F(x, y) \tag{1.1}$$

is defined as an implicit expression of x and y .

That is to see the surface as associated to the levels of the function $F(x, y)$. The surface is intended to be displayed by joining all the level sets. These curves will have previously been obtained by giving different values of z in a given interval $[z_m, z_M]$. Therefore, in this inverse problem, z values for a 2D mesh are not computed. The following sets of points are to be considered instead:

$$S(z) = \{(x, y) | F(x, y) = z\} \tag{1.2}$$

These sets are to be called z -sets.

Depending on the values of z , these z -sets can be empty. Nevertheless, they are usually formed by discrete points or curves.

Each non-empty z -set contains level curves (one or more). These curves can be parametrized by any parameter t :

$$\{(x(t), y(t)) | F(x(t), y(t)) = z\} \quad (1.3)$$

In this project these z -sets are the main object of study. Their qualitative behaviour changes are studied in order to obtain all the necessary information for the 3D plot representation. This kind of inverse problem has been chosen as it is of great use when giving applications.

1.2 A simple example

In this section a simple example is detailed in order to provide a first glance at the problem.

Should the following surface associated to the level function be defined as

$$F(x, y) = (1 - x^2 - y^2)e^{-x^2 - y^2} \quad (1.4)$$

and should $r^2 = x^2 + y^2$ be considered.

The function 1.4 can be expressed in terms of r as

$$f(r) = (1 - r^2)e^{-r^2} \quad (1.5)$$

In order to plot this surface by joining level curves of function 1.5, a previous analytical study is required.

Firstly, the critical points of f must be studied. These are the points where the function has behaviour changes. Hence, they are some of the points where the surface has qualitative changes.

- f has a minimum for $r = \sqrt{2}$ where takes the value $z = -e^{-2}$.
- f presents a maximum for $r = 0$ where takes the value $z = 1$.

f graph decreases from the maximum, as r values increase, and cuts the r -axis, $z = 0$, at value $r = 1$. Once the the minimum is reached, the graph increases without reaching level $z = 0$ for infinite r values. The image of f takes values $z \in [z_m, z_M] = [-e^{-2}, 1]$.

Let us now discuss the shape of the level curves. This surface can be seen as a rotation around the z -axis of f graph for $r \geq 0$. Thus, the level curves obtained are circles centered at the origin and defined by their radius.

The next step to be followed is to discuss those $z \in [z_m, z_M]$ values where behaviour changes of level curves take place. It is important to notice that z values associated to critical values of f are not the only ones where the surface can have qualitative behaviour changes. The z values where the function shows asymptotic behaviour are also to be considered.

The previously mentioned critical points for this specific example will be analysed.

- The minimum value $z_m := -e^{-2}$ has a level curve in the form of a circle of radius $r = \sqrt{2}$. After z_m value, there is a BIRTH of two level curves.
- For $z \in (-e^{-2}, 0)$ z -sets are formed by two level curves: the inner one, C_0 , and the outer one, C_1 . C_0 decreases in radius while C_1 increases in radius to infinity as z level increases.
- At $z = 0$ the inner circle, C_0 does not disappear and has radius $r = 1$. The outer circle increases in radius to infinite as $z \rightarrow 0$ and disappears for $z = 0$. Therefore there is the DEATH of curve C_1 at $z = 0$. In this case there is a qualitative behaviour change of the surface at a z level which is neither a minimum nor a maximum.
- From level $z = 0$ to $z_M := 1$ only C_0 remains and its radius decreases as z level increases.
- For level $z = z_M$, there is a DEATH for C_0 and no other curves for $z > z_M$ exist.

The values $z = z_m$, $z = 0$ and $z = z_M$ are the critical values of the surface. These are the points at which the z -set level curves show qualitative behaviour changes. In this example the only behaviour changes seen are BIRTHS and DEATHS. Nevertheless, other changes such as MERGES or SPLITS may occur at saddle points, which do not appear in this example. In the following sections all these different cases are thoroughly explained.

Once this behaviour study has been made, the next step consists on the computation of each z -set. In order to do so, an approximation of the radius, $r(z)$, at each level is required.

For radius of the inner circles, which have been denoted C_0 , new radii can be updated from the radius of the previous level curve, as there are not big qualitative changes near these curves.

For each level z , the corresponding radius $r(z)$ fulfills the equation

$$f(r) = (1 - r^2)e^{-r^2} = z \quad (1.6)$$

The radius $r(z + dz)$, which is the solution of the next level $z + dz$ equation, can be refined by using the Newton's method. The initial approximation taken is the previous level solution, $r(z)$:

$$r_0 = r(z), \quad r_{k+1} = r_k - \frac{f(r_k)}{f'(r_k)} \quad (1.7)$$

This iterative method is expected to converge to $r(z + dz)$.

Nevertheless, Newton's method can not be applied near radius values where $f'(r) \approx 0$. Such problem occurs at values near the minimum and near the maximum. The way of proceeding at such points is as follows.

Notice that the local expression of f near local extreme values does not include linear terms as $f' = 0$ at such points. Therefore, in order to go from the minimum level, z_m , to the next one, $z_m + dz$, the following expression must be used:

$$z_m + dz \simeq z_m + \frac{1}{2}f''(r_m)(dr)^2, \quad f''(r_m) > 0 \quad (1.8)$$

where the dr estimated correction is

$$dr \simeq \sqrt{\frac{2dz}{f''(r_m)}} \quad (1.9)$$

This expression has been used when dealing with level curves near relative extreme values.

Chapter 2

Analytic study for surface representation

The main aim of this chapter is to explain some details of the mathematical analysis related to surface via level curve representation. This previous analysis is important in order to obtain all of the information related to the function or the tangent fields associated to the level curves.

The scheme of section 1.2 is followed in this chapter but other difficulties and complexities are added to the study.

Firstly, the level curves differential equation systems are introduced. Afterwards, the unitary tangent fields of level curves are explained. Secondly, the stability classification of critical and equilibrium points is detailed. These points are the ones where the surface presents behaviour changes. Thus, they must be properly studied. Once all the information related to behaviour changes of the surface is known, the next steps to be detailed are the preparation and computation of the level curves.

Finally, this chapter introduces the concept of surface slices. Computing the curves in each level is not enough in order to visualize surfaces via level curves. Each curve in a level z must be joined with the following one in the level $z + dz$ in order to obtain a slice. Finally, the surface is displayed by joining these slices. In section 2.4 the mathematical steps used to create the slices are detailed.

2.1 Level curves differential equation systems

In section 1.2 a simple example where all the level curves are circles has been introduced. The aim of this work is to deal with surfaces in which level curves are not circles.

Let the following level curves equation be considered

$$F(x(t), y(t)) = z \quad (2.1)$$

which derived with respect t , results in

$$F_x(x(t), y(t))\dot{x}(t) + F_y(x(t), y(t))\dot{y}(t) = 0 \quad (2.2)$$

From expression 2.2 the level curves tangent field can be obtained:

$$\begin{cases} \dot{x}(t) = \mp F_y(x(t), y(t)) \\ \dot{y}(t) = \pm F_x(x(t), y(t)) \end{cases} \quad (2.3)$$

This tangent field is perpendicular to the gradient of F

$$\begin{cases} \nabla_x F(x(t), y(t)) = F_x(x(t), y(t)) \\ \nabla_y F(x(t), y(t)) = F_y(x(t), y(t)) \end{cases} \quad (2.4)$$

which is normal to the surface.

Should also the unitary tangent field be considered, which allows the use of the arc parameter, s . If the plus sign is chosen in \pm , the unitary tangent field is

$$\begin{cases} x'(s) = -\frac{F_y(x(s), y(s))}{|\nabla F(x(s), y(s))|} \\ y'(s) = \frac{F_x(x(s), y(s))}{|\nabla F(x(s), y(s))|} \end{cases} \quad (2.5)$$

where $|\nabla F(x(s), y(s))|^2 = F_x^2(x(s), y(s)) + F_y^2(x(s), y(s))$.

Each level curve can then be calculated as follows: Firstly, an approximation of the initial point of the curve is calculated. Then, the other points of the curve are computed by numerically integrating the differential equation system 2.5.

2.2 Critical points and equilibrium: stability classification

The aim of this section is to explain how to classify critical points stability. These points can be minimums, maximums or saddle points. In this section their stability is discussed as well as the different types of critical points that may occur: saddle points and centres [7].

The differential equation system 2.5 does not make sense when the gradient of F is 0. This happens at critical points of F , where the tangent field vanishes.

Notice that critical points are those where the tangent field is zero, therefore they are the equilibrium points of the field.

It is important to study these points and their associated critical levels of z as they play an important role in this work. The stability classification enables comprehension of the behaviour of level curves which are near the critical points.

The second derivative of F must be studied in order to analyse the stability of F critical points:

$$\begin{pmatrix} F_{xx} & F_{xy} \\ F_{yx} & F_{yy} \end{pmatrix} \quad (2.6)$$

Where its determinant is: $\Delta = F_{xx}F_{yy} - (F_{xy})^2$.

- If $\Delta > 0$ and $F_{xx}, F_{yy} > 0$ ($F_{xx}, F_{yy} < 0$), the matrix is definite positive (negative). Then the critical point is a minimum (maximum).
- If $\Delta < 0$, the critical point is a saddle point.

The differential matrix of the tangent field is

$$\begin{pmatrix} -F_{xy} & -F_{yy} \\ F_{xx} & F_{xy} \end{pmatrix} \quad (2.7)$$

This matrix must be studied in order to study the linear stability classification of equilibrium points.

Should its characteristic polynomial $\lambda^2 + \Delta$ be considered, where $\Delta = F_{xx}F_{yy} - (F_{xy})^2$ is its determinant. The linear term in λ does not appear as its trace is null. Therefore, the eigenvalues are opposite to each other and are real when $\Delta < 0$ and imaginary when $\Delta > 0$.

- For the case $\Delta < 0$ the equilibrium points are classified as saddle points. Saddle points have associated invariant stable and unstable curves of the tangent field. These curves are considered as singular level curves.
- For the case $\Delta > 0$ the equilibrium points are classified as centres. Each centre is a minimum if $F_{xx}, F_{yy} > 0$ or a maximum if $F_{xx}, F_{yy} < 0$.

Therefore, as the trace of matrix 2.7 is zero, these kind of points are the only ones that can be found in the system. Neither nodes nor foci are studied in this work.

2.3 Level curves

2.3.1 Level curves preparation

In order to simplify this study, all regular level curves are meant to be simple closed curves. Therefore, the chosen applications must satisfy this condition.

In this section the steps to be followed in order to compute each level curve are detailed.

Firstly, a cutting line, $y = y_0$, is given. For each closed curve at a given level, a cutting point (x_0, y_0) , where the curve and $y = y_0$ coincide, is computed. In this way, an initial approximation, (\bar{x}_0, y_0) , is obtained in order to start the curve computation.

Given an approximation for the cutting point, it has to be refined by Newton's method applied to

$$f(x) = F(x, y_0) = z_0 \quad (2.8)$$

That is

$$x_{k+1} = x_k - \frac{f(x_k) - z_0}{f'(x_k)} \quad (2.9)$$

This method is supposed to converge if the first approximation is good enough.

The following lines are dedicated to discuss how to give the first approximation for each level curve. Regular values and critical values are studied separately.

- Regular level curves computation is made by integrating the unitary tangent field. The integration starts at the initial point, (x_0, y_0) , and stops with the next cut with the cutting line, $y = y_0$.
- Singular level curves near a local minimum are computed in the same way. The initial point chosen is a point near the minimum.
- Singular level curves associated to saddle points need a different study before being computed. Let saddle points be seen as equilibrium points of the tangent field. As seen in the previous sections, the characterization of their stability is related to the eigenvalues of the differential matrix of the tangent field. These eigenvalues are opposite to one another

$$\pm\sqrt{-\Delta}$$

where Δ is the determinant of the matrix to be dealt with. This determinant is negative. Therefore, both eigenvalues are real.

The unstable direction, $v = (v_x, v_y)$, of the saddle point is the one associated to the positive eigenvalue, $\lambda = \sqrt{-\Delta}$. It satisfies

$$F_{xx}v_x + (F_{xy} - \lambda)v_y = 0 \quad (2.10)$$

therefore, the direction of v is

$$v = (v_x, v_y) = (\lambda - F_{xy}, F_{xx}) \quad (2.11)$$

The second component of v , F_{xx} , must be used in order to approximate the dx increment with the quadratic expression when dealing with saddle points and minimum points. This is explained in section 3.1.

In order to simplify this study, all singular level curves associated to saddle points are considered to be homoclinic curves. These curves originate from the unstable direction of the saddle point and end tending to the stable direction of the same saddle point. Unstable directions that end up in a different critical point are not studied in this project. Therefore, the chosen applications will satisfy this condition.

In order to compute this homoclinic curves, the tangent field must be integrated starting at a point near the saddle point chosen in the following way

$$(x_0, y_0) = (x^*, y^*) \pm \delta v = (x^*, y^*) \pm \delta(v_x, v_y) \quad (2.12)$$

where (x^*, y^*) is the saddle point to be dealt with.

Notice that this point is on the unstable curve of the saddle point. Therefore, the following computed points of the curve will move away from the saddle point until the cutting line, $y = y^* \mp \delta v_y$, is overcome with the same direction as the one in the first step, v .

As has been seen in previous sections, near a saddle point either a merge of two curves into a single one or the split of a curve into two different ones can occur.

- In a MERGE, two previous curves are joined up into a single singular curve.
- In a SPLIT, two singular curves are created in both sides of the saddle point.

The following curves after a saddle point singular curve must be documented adequately with all the necessary information. The approximation points are obtained by using the quadratic local expression near the saddle point.

2.3.2 Level curves computation

Each level curve must be computed by using numerical integration of the tangent field. The expression for the parameter arc 2.4 is taken under consideration. The method for computing the integration is a Runge-Kutta-Fehlbert method [4].

Given the level z , the starting points for each curve in such level have already been calculated and updated. The integration method starts at the starting points following the tangent field. Under the assumption that all the level curve are simple and closed, the computation of the curve stops when the cutting line is reached in the same direction of the tangent field at the starting point.

Computation of level curves which are not closed might be pursued in future works. In such a case, regular curves should be traced in both ways, integrating them for both positive and negative times. For the not closed level curves case, the stopping criteria has to be different to the one explained in the previous lines. The implementation is easy and it must be discussed more thoroughly. Another extension of this work would be to study examples which include heteroclinic orbits. Singular curves that emerge from a saddle point and end up in a different point or became unbounded are also more difficult to be dealt with.

2.4 Slices preparation

The surface will be displayed by joining the slices between slices of curves at level z and curves at level $z + dz$.

In this section the matching between points at level z and points at level $z + dz$ (or at the same level) is detailed.

Each computed point at a level curve must be associated with a corresponding point at the next level curve as follows:

The computation of this points is made by using a ray in the normal direction to the curve starting from each point (x, y) until the next level, $z + dz$, is reached. This is:

$$F(x + \lambda F_x, y + \lambda F_y) - F(x, y) = dz \quad (2.13)$$

The condition is found by means of a quadratic approximation of the level

function, F . The following quadratic expression results:

$$a\lambda^2 + b\lambda + c \equiv (F_{xx}(F_x)^2 + 2F_{xy}F_xF_y + F_{yy}(F_y)^2)\lambda^2 + ((F_x)^2 + (F_y)^2)\lambda - dz \simeq 0 \quad (2.14)$$

The different scenarios are discussed.

- If $b^2 - 4ac > 0$, the ray will cut the next level at the point

$$(x + \lambda F_x, y + \lambda F_y) \quad (2.15)$$

where λ is the smallest solution of the equation.

- If $b^2 - 4ac < 0$, the ray will not cut the next level but it will probably cut the current level at the point

$$(x + \lambda F_x, y + F_y) \quad (2.16)$$

for λ near $-\frac{b}{a}$.

The initial approximations to λ have to be refined using the secant method or any other iterative method.

Chapter 3

Program implementation

Upon completion of the mathematical analysis of a specific problem, the data must be loaded into the program. This chapter aims at describing the computational work. It has to be seen as a continuation of chapter 2.

Firstly, the storage and organisation of the previously obtained information is detailed. The approach towards operating with slices at critical points has also been explained along with other possible difficulties that may appear.

Secondly, the program structure is detailed. It is important to remark that the aim of this work is to obtain a general visualization application. The aim is to build a program with different modules where the computational work is clearly separated from the specific applied problem.

A C++ environment in Visual Studio has been used in order to implement this project. The specific libraries used for displaying the surface as well as for the simulation controls are described in the following lines.

3.1 Trace for slicing

Let the surface for a level function $F(x, y)$ in an interval of levels $[z_m, z_M]$ be considered. Different values of z between z_m and z_M must be studied in a (vertical) trace of the surface with steps dz that can be changed from one step to the next one. For each level z and its increment dz , the associated slice of $F(x, y)$ will be formed by the computed curve and its 'height' dz .

More specifically, the way of proceeding is detailed in the next lines.

Levels z_0 and $z_0 + dz$, where dz is the increment of z , are to be considered. The chosen dz increment must be the right size in order to provide a good visualization, neither too small nor too big. Once z_0 and $z_0 + dz$ have been considered, a slice which will join these two curves will be taken into account. Once this step

has ended, z_0 and $z_0 + dz$ levels are changed to the next ones. As has been seen in the previous sections, this study deals with two kind of points: regular values and critical values.

These two different kinds will be treated separately as follows:

- At regular values z_0 , far from critical values, level curves at z_0 level have a natural continuation as curves at $z_0 + dz$ level. This implies that the surface near these values has soft changes which are to be dealt with easily.
- At critical values, which will be referred to as z^* from now on, greater qualitative changes of the surface occur. Some of the level curves may disappear (death), some others may appear (birth), some others may join (merge) or some others may separate (split). For these cases special attention and treatment will be needed.

The case near a critical value, z^* , with $z_0 < z^*$ and $z_0 + dz > z^*$ must be studied in more depth. In this case the update process of z_0 must be performed in two steps. Firstly, level z^* is achieved by considering $dz = z^* - z_0$. Secondly, starting at the critical value, z^* , and considering the previous dz .

Therefore, in these cases two slices are taken into account: the first one, at a level between z_0 and z^* , and the second one, at a level between z^* and $z^* + dz$.

The computation of slices near critical values for the different situations that may occur is organize and prepared as follows:

- Starting at a critical value.

Two different cases must be taken into account depending on whether the critical value is a minimum or a saddle.

For each level curve which follows the previous one, the cutting point must be updated and the respective level curve is to be computed and saved appropriately as a slice with its increment dz .

For each new level curve, the corresponding singular level curve must computed and saved appropriately its slice with increment dz . The cutting point for the new level curve must be found as follows:

- If the new curve appears after a relative minimum, which means that a BIRTH takes place, the singular level curve might be a little curve around the minimum. In such case the approximation of the new cutting point must be computed by using the local quadratic expression

$$dx \simeq \sqrt{\frac{2dz}{F_{xx}}} \quad (3.1)$$

- If the new curve is near a saddle point, this curve will either be the result of a MERGE of two previous curves or a SPLIT of one previous curve into two new curves. In such a case, the singular level curve (one if there is a MERGE or two if there is a SPLIT) must be found by following the unstable direction near the saddle point. The computation stops when new computed points are near the saddle point following its stable direction. The approximation of the new cutting point must be computed by using the local quadratic expression 3.1.

- Arriving at a critical value.

For each level curve, the new cutting point must be updated and the corresponding level curve is computed. Its slice must be saved appropriately with increment $z^* - z_0$. The level curve continuation at the critical point must be prepared.

- Otherwise.

For each level curve, the update the cutting point must be done as well as the computation of the corresponding level curve. Its slice must be saved with dz increment.

3.2 Bifurcation diagram

In order to compute the 3D surface a bifurcation diagram for the level curves is needed. It is important that all the information of the level curves is provided at each level in each trace of slices.

In section 4.8.7 different bifurcation diagrams for the XPCR3BP are detailed. For this specific application there is more than one bifurcation diagram.

This section explains how each of the diagrams in section 4.8.7 are computed. In the XPCR3BP application sections the bifurcation in α parameter, which leads to the different bifurcation diagrams of the level curves, is explained. This two different bifurcation diagrams should not be mixed up or confused.

The bifurcation diagram depending on z values must contain all the necessary information related to critical values and curves evolution. In order to overcome these difficult critical point levels and continue beyond. Its implementation is performed in such a way that it contains all the information needed to do a trace of the surface slices.

The following information is contained in the bifurcation diagrams:

- A list of the $n + 1$ critical values, Z_j , $j = 0, 1, \dots, n$ and the partition of the interval $[z_m, z_M]$ in n parts: $[Z_j, Z_{j+1}]$, $j = 0, 1, \dots, n - 1$.
- For each critical value, Z_j , the following information for each of the curves C_{jk} in this part j is needed.
 - The cutting line, $y = y_0$, for each one of the curves C_{jk} in this part j .
 - An approximation of the abscissa x_0 at the cutting point with this cutting line to be updated for the levels Z up to the following critical level.
 - The directions (v_x, v_y) explained in section 2.3 in order to continue from a minimum or a saddle point.
 - The index k for the continuation of curves from the current part to the following one.

Figure 3.1 shows the code lines where the different used structures are defined. Let them be explained:

- Zm and ZM stand for the extremes of the z interval $[z_m, z_M]$.
- $Z0$ and dZ are the current z value and increment respectively.
- ZC are the critical levels which determine the partition. JC is the associated extended Jacobi constant. ZCn is the number of subintervals in the partition.
- $Zy0$ is the cutting line and $Zx0$ the cutting point of the cutting line with the curve.
- Zvx and Zvy are the saddle directions. Zvx is only used at saddle points. Therefore, for minimum's $Zvx = -1$ and for cuspids $Zvx = -2$.
- Zk indicates in which curve of the next part a curve continues after crossing the critical level. If a curve does not continue in the next part, the respective component of this vector takes value -1 . If the curves continue after crossing critical levels.
- ZLS is the vector where the packed z -level curves with dz increment (strips) are stored. It contains (x, y, z, dz) information for each computed point.

The number of components of the vectors is the number of curves for each subinterval of the partition in $[z_m, z_M]$. The bifurcation diagram contains this information.

The initialization of these structures is made in the code module related to the specific problem to be applied.

```

Interval of levels Z
double Zm, ZM;
Current values Z0 and increment dZ
double Z0, dZ;
Bifurcation diagram
Critical levels: ZC partition
vector<double> ZC;
vector<string> JC;
int ZCn;
Part j: Z-values from ZC[j] to ZC[j+1]
Cut lines y=y0
vector<vector<double>> Zy0;
Previous x (set up)
vector<vector<double>> Zx0;
saddle directions (unless Zvx=-1: minimum, Zvx=-2: cusp)
vector<vector<double>> Zvx;
vector<vector<double>> Zvy;
curve continuation when crossing critical levels
vector<vector<int>> Zk;
Z-Level sets ZLS[j] formed by components ZLS[j][k]
of packed Z-Level curves/strips of points (X,Y,Z,dZ)
vector<vector<vector<double>>> ZLS;

```

Figure 3.1: Code lines with structures used in the bifurcation diagrams.

Most of this information is used when the trace of the surface approaches and reaches critical values in order to update the information related to level curves beyond the singular curves.

For levels between critical values, the bifurcation diagram is used to update the approximations of the abscissa of the intersections point of the curves with the cutting lines.

It is important to remark that each computed level curve is stored in a vector of points, C_{jk} , as a slice. That is a set of points (x, y, z, dz) indicating the coordinates as well as the increment to the next level.

For each part j of the partition and each different component k a pack of curves $C[j][k]$ will be stored in ZLS vector. This vector is filled as the trace for slicing is done. For given j and k values, from each critical level $ZC[j]$ to the next level $ZC[j+1]$, the computed curves must be stored in different slices from the critical level $ZC[j]$ to the next level $ZC[j+1]$. In this way, all the computed curves can be displayed at any time of the trace.

Notice that once the partition of $[z_m, z_M]$ is done, every level in a part has the same number of components.

3.3 Curves and slices display

The stored slices can be displayed in four different ways through the trace:

- As curves of the current level.
- As curves from the starting level to the current level.
- As slices of the current level.
- As slices from the starting level to the current level.

Each curve is displayed as a polygonal which joins all of its points. In order to clearly visualize the z level of each curve, an rgb colour is associated to each level z . The polygonal joinings can be displayed with `glBegin(GL_LINE_STRIP)` in an implementation that uses the *OpenGL* library. Upon completion of the curve computation and storage, the next step is to display the slices. They are displayed as a strip which is between computed points of a curve at a level z and associated points according to section 2.4 of the following curve at level $z + dz$. In order to do so, for each point at level z , the corresponding point at the next level (or in the same level) is computed. The strips can be displayed with `glBegin(GL_QUAD_STRIP)` in an implementation that uses the *OpenGL* library.

3.4 Simulation

The simulation has been implemented using *OpenGL* [6] and *FastLightToolkit* (FLTK). These are libraries used for implementing a graphical user interface with controls to plot 3D surfaces.

3.5 Program organization

The resulting C++ code has been structured as follows:

- **LC_Control.cpp**: This module contains the main function as well as the FLTK related functions to produce the simulation interface and controls.
- **LC_Compute.cpp**: This module computes the level curves. It contains a compute function that needs the information related to the bifurcation diagram in the interval of z levels. In this way, all the levels, including the critical ones, can be computed. For each z level, the cutting point is calculated and refined by calling the Newton's method. Then, RKF method is

called in order to compute the curves in this level. The only specific information related to the XPCR3P application is the tangent field needed for the level curves computation.

- **LC_View.cpp**: this module contains the code related to level curves and slices display. As well as the code for solving the equation for the normal ray in order to cut the next or the same curve. As has previously been explained, this step is essential for obtaining the strips corresponding to the slices. This file also prints to file the computed slices and plots them from file.
- **RKF.cpp**: This file contains the code for Runge-Kutta 4-5 (RK45) method and Runge-Kutta-Fehlberg 7-8 (RKF78) method. One of these methods can be chosen in each application.
- **LC_XR3BP.cpp**: This file contains the specific information related to the application to the XPCR3P problem.

These different modules are connected with each other. Firstly, all of the information related to the specific problem is collected and implemented in LC_XR3BP.cpp. In this document, an application called Applnit is the one that contains all the information to initialize the slices trace. After this, LC_compute.cpp contains the code related to the slices packs storage. The code in this file is called by the user when z levels move forward through the trace to compute and store the corresponding slices. The code in LC_View.cpp shows the computed slices. In these modulus more than one visualization mode is implemented. Starting at z_m , and moving until a level z , the current curve, or all curves until z , or the current slice, or all the surface until z can be displayed. Finally, an option for writing in a file is implemented. In this way, the simulator will contain enough displaying options in order to visualize the surface. These different view options are detailed in section 5.1.1.

Chapter 4

Global representation of the zero-velocity curves in the XPCR3BP

The aim of this chapter is to introduce the Extended Planar and Circular Restricted 3-Body Problem (XPCR3BP). The main purpose is to prepare all of the information related to this specific problem in order to provide an application of the surface visualization simulation explained in the previous chapter.

This chapter firstly introduces the extended two body problem as it is related with the XPCR3BP. Afterwards, the extended potentials related to the XPCR3BP are introduced. In order to simplify the equations non-dimensional units and the Hamiltonian formulation of the problem must be studied. A coordinate system change is chosen: the sinodical coordinate system. In this way an autonomous Hamiltonian formulation of the equations of motion of the third body are to be obtained. This previous work is necessary in order to obtain a Hamiltonian field, which admits a first integral.

After this, all the information needed for the surface via level curves visualization is analyzed. The following step is to study the equilibrium points, which are called Lagrangian points. Afterwards, zero-velocity curves and extended Jacobi constants must be studied. These curves are the ones that will be plotted. Once these curves have been obtained the steps to be followed are the same as the ones explained in chapter 2 for the analytic part and in chapter 3 for the programming part.

The main aim of this work is to plot 3D surfaces via level curves associated to the zero-velocity curves that can be considered as levels of a function related with

the (extended) Jacobi constants of the problem in sinodic coordinates. Therefore, the 3-body problem will be explained without many details. It will not be studied in depth and only the most relevant steps in obtaining the equations will be explained.

This project is the continuation of a previous final degree project: Problema extendido de tres cuerpos, restringido y circular (Erik Lopez Alonso) [8]. Many of the information found in this chapter has been obtained from this previous work. In this chapters the following references have also been used: [1], [2], [3], [5].

4.1 The extended two body problem

Let us introduce the notion of the two body problem, which is simpler than the one we want to study. In contrast with the three body problem, in the two body problem both energy and momentum remain preserved separately. Therefore, it admits a general analytical solution.

For the study of the three body problem a different approach must be used in order to find the preserved magnitude. In this case this magnitude is not the energy and momentum but the Jacobi integral, which will be explained and studied in the following sections.

Despite their differences, the two body problem will be of great use as it will help us understand the three body problem before giving a deeper insight of it.

Let two bodies with masses M_1 and M_2 with $M_1 \geq M_2$ be considered. These two bodies are called the primary and secondary bodies. Let us consider an inertial reference frame in which \vec{R}_1 and \vec{R}_2 represent the vectors of the bodies position respectively. $\vec{R} := \vec{R}_2 - \vec{R}_1$ is the vector between the two bodies with modulus R . The forces involved in this problem are attractive forces with modulus $GM_1M_2\bar{R}^\alpha$. The case $\alpha = -2$ corresponds to the classical gravitational force.

The two-body problem can be reduced to a Kepler's problem, where both bodies will be affected by central forces.

The center of masses $(\bar{X}_0, \bar{Y}_0) = \frac{M_1\vec{R}_1 + M_2\vec{R}_2}{M_1 + M_2}$ moves at constant velocity. Therefore, an inertial frame of reference with origin (\bar{X}_0, \bar{Y}_0) can be chosen: the barycentric sidereal reference system.

The problem that studies the variation of the relative position vector (\bar{X}, \bar{Y}) of the primary body in relation to the secondary body is known as The extended Kepler's problem. It involves central attractive forces of modulus

$$F_\alpha(\bar{R}) = \kappa\bar{R}^\alpha \quad (4.1)$$

where $\kappa = G(M1 + M2) \equiv GM$.

The equations of motion are:

$$\begin{cases} \frac{d^2\bar{X}}{dt^2} = -\kappa\bar{X}\bar{R}^{\alpha-1} \\ \frac{d^2\bar{Y}}{dt^2} = -\kappa\bar{Y}\bar{R}^{\alpha-1} \end{cases} \quad (4.2)$$

where $\bar{R}^2 = \bar{X}^2 + \bar{Y}^2$.

The position of the two bodies is now written as

$$\begin{cases} (\bar{X}_1, \bar{Y}_1) = (\bar{X}_0, \bar{Y}_0) + \frac{M_2}{M_1+M_2}(\bar{X}, \bar{Y}) \\ (\bar{X}_2, \bar{Y}_2) = (\bar{X}_0, \bar{Y}_0) + \frac{M_1}{M_1+M_2}(\bar{X}, \bar{Y}) \end{cases} \quad (4.3)$$

where (\bar{X}_0, \bar{Y}_0) is considered to be in the origin of coordinates.

4.2 The extended potentials and their circular orbits

The central forces of the extended Kepler's problem has associated extended central potentials:

$$V_\alpha(\bar{R}) = \begin{cases} \frac{\kappa}{\alpha+1}(\bar{R}^{\alpha+1} - 1) & \text{if } \alpha \neq -1 \\ \kappa \ln(\bar{R}) & \text{if } \alpha = -1 \end{cases} \quad (4.4)$$

Notice that the origin of potentials has been fixed to $\bar{R} = 1$ instead of $\bar{R} = \infty$ in order to have consistent extended potentials.

In extended Kepler problems the angular momentum, K , and the energy, E , are both first integrals of the system. Which means that both magnitudes remain constant along the orbits.

When the orbits are circular with radius \bar{R}_c the angular momentum is $K = K_c = n\bar{R}_c$. Where n is the angular velocity which is constant. Circular orbits take place for \bar{R}_c which minimize or maximize the extended effective potentials associated to

$$V_\alpha(\bar{R}) = \begin{cases} \frac{K^2}{2\bar{R}^2} + \frac{\kappa}{\alpha+1}(\bar{R}^{\alpha+1} - 1) & \text{if } \alpha \neq -1 \\ \frac{K^2}{2\bar{R}^2} + \kappa \ln(\bar{R}) & \text{if } \alpha = -1 \end{cases} \quad (4.5)$$

For circular orbits with radius $\bar{R} = \bar{R}_c$, $K = K_c = n\bar{R}_c^2$ where n is the angular velocity which is constant. These $\bar{R} = \bar{R}_c$ are those where 4.5 derivative vanishes:

$$-\frac{K_c^2}{\bar{R}_c^3} + \kappa\bar{R}_c^\alpha = -n^2\bar{R}_c^\alpha + \kappa\bar{R}_c^\alpha = 0 \quad (4.6)$$

The extended Kepler third law relates the radius \bar{R}_c with the angular velocity n :

$$n^2 \bar{R}_c^{1-\alpha} = \kappa \quad (4.7)$$

This expression for the classical gravitational case is

$$n^2 \bar{R}_c^3 = \kappa \quad (4.8)$$

The effective extended potentials are depicted in figure 4.1 for a particular interesting case.

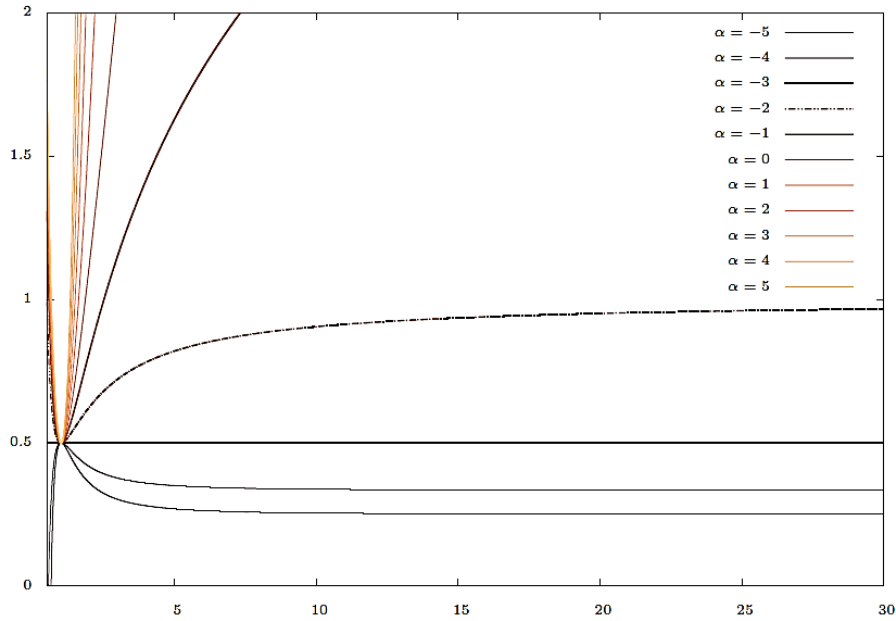


Figure 4.1: Extended potentials $V_\alpha(\bar{R})$, are plotted for $\alpha = -5 \div 5$ for $K_c = 1$ and $\kappa = 1$. It has logarithmic behaviour for $\alpha = -1$ and it vanishes for $\alpha = -3$. The functions has a minimum for $\alpha > 3$ and a maximum for $\alpha < 3$ at $\bar{R} = \mathbb{R}_c = 1$. The classical gravitational has been represented with a dashed line.

4.3 The extended planar and circular three-body problem

The aim of this section is to introduce the extended planar and circular restricted 3-body problem. The motion of the primary and the secondary bodies will be restricted in order to describe circular orbits around the centre of masses. The orbits to be described are circular, with constant angular velocity n and radius \bar{R}_c , which are the orbits of the associated extended Kepler problem.

The two primary bodies remain at distance $d = \bar{R}_c$ and describe the following circular orbits:

$$(mD \cos(n\bar{t}), mD \sin(n\bar{t})), ((m-1)D \cos(n\bar{t}), (m-1)D \sin(n\bar{t})) \quad (4.9)$$

where the initial positions chosen are $(mD, 0)$ and $((m-1)D, 0)$ where $M = M_1 + M_2$, $m = \frac{M_2}{m}$ and $1 - m = \frac{M_1}{M}$.

The extended planar and circular restricted 3-body problem (XPCR3BP) analyzes the movement of a third body under the interaction of the two primary bodies. This body describes circular orbits which are at the plane described by the primary bodies movement. The restricted adjective refers to a third body which does not disturb the circular orbits of the primary bodies.

The third body differential equations of motion are:

$$\begin{cases} \frac{d^2\bar{X}}{d\bar{t}^2} = -GM((1-m)(\bar{X} - mD \cos(n\bar{t}))\bar{R}_1^{\alpha-1} + m(\bar{X} - (m-1)D \cos(n\bar{t}))\bar{R}_2^{\alpha-1}) \\ \frac{d^2\bar{Y}}{d\bar{t}^2} = -GM((1-m)(\bar{Y} - mD \sin(n\bar{t}))\bar{R}_1^{\alpha-1} + m(\bar{Y} - (m-1)D \sin(n\bar{t}))\bar{R}_2^{\alpha-1}) \end{cases} \quad (4.10)$$

Where

$$\begin{aligned} \bar{R}_1^2 &= (\bar{X} - mD \cos(n\bar{t}))^2 + (\bar{Y} - mD \sin(n\bar{t}))^2 \\ \bar{R}_2^2 &= (\bar{X} - (m-1)D \cos(n\bar{t}))^2 + (\bar{Y} - (m-1)D \sin(n\bar{t}))^2. \end{aligned}$$

4.4 The XPCR3BP in non-dimensional units

The aim of this section is to simplify the equations of motion by choosing the appropriate units.

The following scaling transformations in lengths and time is chosen:

$$(\bar{X}, \bar{Y}) = D(X, Y), \quad n\bar{t} = t \quad (4.11)$$

and using the extended Kepler's third law, $n^2D = GMD^\alpha$, the equations are simplified to:

$$\begin{cases} \frac{d^2X}{dt^2} = -[(1-m)(X - m \cos(t))r_1^{\alpha-1} + m(X - (m-1) \cos(t))R_2^{\alpha-1}] \\ \frac{d^2Y}{dt^2} = -[(1-m)(Y - m \sin(t))r_1^{\alpha-1} + m(Y - (m-1) \sin(t))R_2^{\alpha-1}] \end{cases} \quad (4.12)$$

Once the orbits in the scaled system are known, the real orbits can be reintroduced:

$$(\bar{X}(t), \bar{Y}(t)) = D(X(n\bar{t}), Y(n\bar{t})) = D(X(t), Y(t)) \quad (4.13)$$

The main reductions of this scaling change to non-dimensional units are:

- The unit of mass is now the sum of the primary bodies. Therefore, the masses are: $1 - m, m$.
- The distance between primary bodies is now the unit of distance and therefore it remains constant.
- The angular velocity is now unitary. The primary bodies take a time 2π to complete an orbit. Therefore the time has been chosen in order to fulfill this property.
- The gravitational constant does not appear in the equations because it is unitary.
- Circular motion: it has been reduced to

$$me^{it} = (m \cos(t), m \sin(t)), (m - 1)e^{it} = ((m - 1) \cos(t), (m - 1) \sin(t)) \quad (4.14)$$

where the initial positions at $t = 0$ have been taken at $(m, 0)$ and $(m - 1, 0)$.

The extended Kepler's problem with non-dimensional units corresponds to the problem chosen in figure 4.1 where $\kappa = GM = 1$ and $K = 1$ that describes circular orbits with radius $R_c = 1$ and angular velocity $n = 1$.

For particular known cases with values for the radius D (meters) and the period T (seconds) the non-dimensional units of time, length, are respectively $\frac{T}{2\pi}$ seconds, D meters and the total mass $M = \frac{n^2 R_c^{1-\alpha}}{G}$ kilograms with angular velocity $n = \frac{2\pi}{T}$.

The following examples enable easier understanding of the non-dimensional units:

- In a Sun-Jupiter system: The (almost constant) distance between the Sun and Jupiter $D = 778547200$ km is taken as distance unit. It is called the astronomic unit (a.u.). The time unit taken is the Jupiter period $T = 11.86$ years divided by 2π . The total mass unit is approximately the sun mass $\frac{n^2 D^3}{G} = \frac{4\pi^2 D^3}{T^2} = 1.988 \cdot 10^{30}$.
- In a Sun-Earth system: The (almost constant) distance between the Sun and the Earth $D = 149598261$ km is taken as distance unit. The time unit taken is the Earth period $T = 1$ year divided by 2π . The total mass unit is approximately the Sun mass $\frac{n^2 D^3}{G} = \frac{4\pi^2 a^3}{T^2} = 1.988 \cdot 10^{30}$ kg.

4.5 Hamiltonian formulation of the XPCR3P in sinodic coordinates

In this section the baricentric sinodical coordinate system is introduced. This system rotates around the origin of coordinates with unitary angular velocity with the primary and secondary bodies. In this way, the primary bodies are fixed at positions $(m, 0)$ and $(m - 1, 0)$.

The following autonomous Hamiltonian function results

$$H(x, y, p_x, p_y) = \frac{1}{2}(p_x^2 + p_y^2) - (xp_y - yp_x) + v_{\alpha, m}(x, y) \quad (4.15)$$

and the potentials are

$$v_{\alpha, m}(x, y) = \begin{cases} (1 - m)\frac{1}{\alpha+1}(r_1^{\alpha+1} - 1) + m\frac{1}{\alpha+1}(r_2^{\alpha+1} - 1) & \text{if } \alpha \neq -1 \\ (1 - m)\ln(r_1) + m\ln(r_2) & \text{if } \alpha = -1 \end{cases} \quad (4.16)$$

where $r_1^2(t) = (x - m)^2 + y^2$ and $r_2^2(t) = (x - (m - 1))^2 + y^2$.

The extended sinodical potentials can be written

$$v_{\alpha, m}(x, y) \equiv (1 - m)v_{\alpha}(r_1) + mv_{\alpha}(r_2) \quad (4.17)$$

where

$$v_{\alpha}(r) = \begin{cases} \frac{1}{\alpha+1}(r^{\alpha+1} - 1) + m\frac{1}{\alpha+1} & \text{if } \alpha \neq -1 \\ \ln(r) & \text{if } \alpha = -1 \end{cases} \quad (4.18)$$

The Hamiltonian equations of motion of the third body respect to time t are

$$\begin{cases} \dot{x} = p_x + y & \dot{p}_x = -(1 - m)(x - m)r_1^{\alpha-1} - m(x - (m - 1))r_2^{\alpha-1} \\ \dot{y} = p_y - x & \dot{p}_y = -(1 - m)(y - m)r_1^{\alpha-1} - m(y - (m - 1))r_2^{\alpha-1} \end{cases} \quad (4.19)$$

4.6 Equilibrium points of the extended problem

Since the obtained potential depends on the velocity, the problem can no be solved by studding the effective potential. Therefore, Lagrangian points linear stability will be taken into account.

Definition 4.1. *The points where the sinodical Hamiltonian field vanishes are called Lagrangian points. Their equilibrium equations are:*

$$\begin{cases} x - (1 - m)(x - m)r_1^{\alpha-1} - m(x - m + 1)r_2^{\alpha-1} = 0 \\ y - (1 - m)yr_1^{\alpha-1} - myr_2^{\alpha-1} = 0 \end{cases} \quad (4.20)$$

The sinodical coordinate sistem with unitary angular velocity has been chosen. Therefore this equilibrium means that the attractive gravitational force and the centrifugal force are counterbalanced.

4.6.1 Equilibrium points classification

- **Equilateral equilibrium points:** These are two points that form equilateral triangles with the primary and the secondary bodies: $L_4 = (m - \frac{1}{2}, \frac{\sqrt{3}}{2})$, $L_5(m - \frac{1}{2}, -\frac{\sqrt{3}}{2})$. They exist for all $\alpha \neq 1, m \neq 0$.
- **Collinear equilibrium points:** These points are placed at x -axis.
 - **Collision solutions:** collision points are placed at the positions of the primary and the secondary bodies: $L_{-1} = (a_{-1}(\alpha) + m, 0)$ and $L_0 = (a_0(\alpha) + m, 0)$, where $a_{-1}(\alpha) = -1$ and $a_0(\alpha) = 0$. They become singularities for all $\alpha < 0$.

The following collinear equilibrium points can be placed in three different intervals of the x -axis: $L_1 = (a_1 + m, 0)$ between the two primary bodies; $L_2 = (a_2 + m, 0)$ beyond the secondary body; $L_3 = (a_3 + m, 0)$ beyond the primary body.

The solutions a_1, a_2 and a_3 depend on α :

- **Solution $a_1(\alpha, m)$:** The solution $a_1(\alpha, m) \in (0, 1)$ exists for all $\alpha \leq \frac{1}{1-m}$ and $\alpha \geq \frac{1}{m}$. For $\alpha = \frac{1}{1-m}$ it coincides with $a_2(\alpha, m)$ and with $a_{-1}(\alpha, m)$. For $\alpha = \frac{1}{m}$ it coincides with $a_0(\alpha) = 0$ and with $a_3(\alpha, m)$.
- **Solution $a_2(\alpha, m)$** The solution $a_2(\alpha, m) \in (-1, 0)$ exists for all $\alpha \leq \frac{1}{1-m}$. For $\alpha = \frac{1}{1-m}$ it coincides with $a_1(\alpha, m)$ and with $a_{-1}(\alpha) = -1$.
- **Solution $a_3(\alpha, m)$** The solution $a_3(\alpha, m) \in (1, \infty)$ exists for all $\alpha \leq \frac{1}{m}$. For $\alpha = \frac{1}{m}$ it coincides with $a_0(\alpha) = 0$ and with $a_2(\alpha, m)$.

Table 4.1 summarizes all the information previously discussed in this section. Each collinear equilibrium point comes with its corresponding equilibrium equation and with its corresponding α interval for which they exist.

Table 4.1: Collinear equilibrium points, the corresponding equilibrium equations and α intervals.

Equilibrium points	Equation	Interval
$L_{-1} = (-1 + m, 0)$		$\alpha \geq 0$
$L_0 = (m, 0)$		$\alpha \geq 0$
$L_1 = (a_1 + m, 0)$	$a_1 + m + (1 - m)(-a_1)^\alpha - m(a_1 + 1)^\alpha = 0$	$\alpha < \frac{1}{(1-m)}, \frac{1}{m} < \alpha$
$L_2 = (a_2 + m, 0)$	$a_2 + m + (1 - m)(-a_2)^\alpha + m(a_2 - 1)^\alpha = 0$	$\alpha < \frac{1}{1-m}$
$L_3 = (a_3 + m, 0)$	$a_3 + m - (1 - m)(a_3)^\alpha - m(a_3 + 1)^\alpha = 0$	$\alpha < \frac{1}{m}$
$L_1 = L_2 = L_3$	$a_1 = a_2 = -1$	$\alpha = \frac{1}{1-m}$
$L_3 = L_1 = L_0$	$a_3 = 0$	$\alpha < \frac{1}{m}$

4.7 Extended Jacobi constants and zero-velocity curves

In section 4.5 the Hamiltonian formulation for the motion of the third body has been obtained. It is now a first integral of the system.

In this section zero-velocity curves will be described. They are the curves that will be seen as level curves of the surface to be represented.

Definition 4.2. *The extended Jacobi's integral is defined as $-2H$. Its constant values, $J(\alpha, m)$ are called extended Jacobi constants.*

Let the Hamiltonian be rewritten in terms of positions and velocities by substituting the expressions of moments $p_x = \dot{x} - y$ and $p_y = \dot{y} + x$ in the equation 4.15. The following expression results:

$$\begin{aligned}
 -2H(x, y, \dot{x}, \dot{y}) &= (1 - m)(r_1^2 - 2v_\alpha(r_1)) + \\
 m(r_2^2 - 2v_\alpha(r_2)) - m(1 - m) - (\dot{x}^2 + \dot{y}^2) &= J(\alpha, m)
 \end{aligned} \tag{4.21}$$

See appendix A to see the case of Jacobi constants for the gravitational case, $\alpha = -2$.

Definition 4.3. *For each extended Jacobi constant the extended Hill's region is defined as*

$$r^2 - 2v_{\alpha, m}(r) = (1 - m)(r_1^2 - 2v_\alpha(r_1)) + m(r_2^2 - 2v_\alpha(r_2)) - m(1 - m) \geq J(\alpha, m) \tag{4.22}$$

The movement in the sinodic coordinates is restricted in this region.

Definition 4.4. *The curves that delimit Hill's regions are called zero-velocity curves. Their equation is*

$$r^2 - 2v_{\alpha,m}(x, y) = (1 - m)(r_1^2 - 2v_{\alpha}(r_1)) + m(r_2^2 - 2v_{\alpha}(r_2)) - m(1 - m) = J(\alpha, m) \quad (4.23)$$

Zero-velocity curves can be seen as level curves of the function

$$\Omega_{\alpha,m}(x, y) = \frac{1}{2}(x^2 + y^2) - v_{\alpha,m}(x, y) = \frac{1}{2}r^2 - (1 - m)v_{\alpha}(r_1) - mv_{\alpha}(r_2) \quad (4.24)$$

For a given value $J(\alpha, m)$, these curves are defined by

$$JVC(J(\alpha, m)) = \{(x, y) | 2\Omega_{\alpha,m}(x, y) = J(\alpha, m)\} \quad (4.25)$$

The zero-velocity curves for different extended Jacobi constants are usually plotted in a 2D graph. The aim of this work is to go a step further and obtain a 3D plot. In order to do so, zero-velocity curves will be seen as level curves of the function $\Omega_{\alpha,m}$.

4.8 Analysis of $\Omega_{\alpha,m}$ function

An expression for $\Omega_{\alpha,m}$ has been found. This is the function that must be studied in order to give an application for surface representation via level curves. The following sections have the aim to make an accurate analysis of the zero-velocity curves seen as level curves of $\Omega_{\alpha,m}$.

The analysis will be structured as follows:

- The first analysis studies the points of $\Omega_{\alpha,m}$ where level curves have a characteristic behaviour. These are the critical and cuspidal points of $\Omega_{\alpha,m}$ which will be referred to as characteristic points from now on.
- The second analysis studies the extended Jacobi constant values ordering. For a given m value, changes in the qualitative behaviour of zero-velocity curves depending on different α values must be studied. In order to do so, the values of α for which extended Jacobi constant values coincide at characteristic points must be discussed. Therefore, bifurcation diagrams of Jacobi constants and equilibrium points depending on α will be obtained.
- The third analysis studies Hill's regions qualitative evolution in terms of the extended Jacobi constant. Bifurcation diagrams containing all the needed information of level curves evolution are to be given.

4.8.1 Characteristic points of $\Omega_{\alpha,m}$

Critical points of $\Omega_{\alpha,m}$ and their extended Jacobi constants play an important role in the analysis of zero velocity curves.

Definition 4.5. *The critical points of $\Omega_{\alpha,m}$ satisfy*

$$\begin{cases} D_x \Omega_{\alpha,m}(x, y) = x - (1 - m)(x - m) - (r_1^{\alpha-1} - m(x - m + 1)r_2^{\alpha-1}) = 0 \\ D_y \Omega_{\alpha,m}(x, y) = y - (1 - m)yr_1^{\alpha-1} - myr_2^{\alpha-1} = 0 \end{cases} \quad (4.26)$$

These are the points where the derivative of $\Omega_{\alpha,m}$ vanishes.

This condition is the same as Lagrange points condition, where the Hamiltonian field vanishes. This happens because Lagrange points are critical points of $\Omega_{\alpha,m}$.

Let the behaviour in such points depending on different α values be studied.

Critical points can be classified by studying $\Omega_{\alpha,m}$ second derivative, the Hessian matrix $D^2\Omega_{\alpha,m}(x, y)$ is

$$\begin{pmatrix} 1 - (1 - m)\left[1 + (\alpha - 1)\frac{(x-m)^2}{r_1^2}\right]r_1^{\alpha-1} & -(1 - m)(\alpha - 1)(x - m)yr_1^{\alpha-3} \\ -m\left[1 + (\alpha - 1)\frac{(x-m+1)^2}{r_2^2}\right]r_2^{\alpha-1} & -m(\alpha - 1)(x - m + 1)yr_2^{\alpha-3} \\ -(1 - m)(\alpha - 1)(x - m)yr_1^{\alpha-3} & 1 - (1 - m)\left[1 + (\alpha - 1)\frac{y^2}{r_1^2}\right]r_1^{\alpha-1} \\ -m(\alpha - 1)(x - m + 1)yr_2^{\alpha-3} & -m\left[1 + (\alpha - 1)\frac{y^2}{r_2^2}\right]r_2^{\alpha-1} \end{pmatrix} \quad (4.27)$$

4.8.2 Collision points

The collision points, $L_0 = (m, 0)$ and $L_{-1} = (m - 1, 0)$, are to be classified as cuspidal, peaks or critical points. Where a point is singular if the function is not defined in the point; a point is cuspidal if the derivatives F_x, F_y in the point are not defined; and a point is a peak is the second derivatives F_{xx}, F_{xy} and F_{yy} in the point are not defined.

Extended Jacobi constants for collision points are:

$$J_0(\alpha, m) = 2\Omega_{\alpha,m}(L_0) = (1 - m)\frac{2}{\alpha + 1} + m^2 \quad (4.28)$$

$$J_{-1}(\alpha, m) = 2\Omega_{\alpha,m}(L_{-1}) = m\frac{2}{\alpha + 1} + (1 - m)^2 \quad (4.29)$$

For $\alpha < -1$ these two points are singularities of the Hamiltonian field. Therefore, let $\alpha > -1$ be considered.

- **Case $\alpha < -1$:** L_0 and L_{-1} are singular points as they are singularities of the Hamiltonian field and $\Omega_{\alpha,m}$ is unbounded.
- **Case $-1 < \alpha < 0$:** For $\alpha < 0$, L_0 and L_{-1} are singularities of the Hamiltonian field and therefore cannot be classified as equilibrium points. However, the derivatives of $\Omega_{\alpha,m}$ remain unbound for $-1 < \alpha < 0$, therefore collision points are cuspidal points of $\Omega_{\alpha,m}$ for such alpha values.
- **Case $0 \leq \alpha < 1$:** for values $\alpha \geq 0$ points L_0 and L_{-1} satisfy the equation 4.26, they are critical points of $\Omega_{\alpha,m}$. However, for $0 \leq \alpha < 0$, $D^2\Omega_{\alpha,m}(L_0)$ and $D^2\Omega_{\alpha,m}(L_{-1})$ are unbounded. Therefore, in this interval collision points can not be classified as critical points strictly due to the singularity in $\Omega_{\alpha,m}$ second derivatives. They can be classified as a softer kind of cuspidal points which are called peak points.
- **Case $\alpha \geq 1$:** this is the case which requires wider study.

For the primary collision, $L_0 = (m, 0)$, the Hessian matrix is the diagonal matrix:

$$D^2\Omega_{\alpha,m}(L_0) = \begin{pmatrix} 1 - m\alpha & 0 \\ 0 & 1 - m \end{pmatrix} \quad (4.30)$$

Where $(1 - m) > 0$ if $\alpha < \frac{1}{m}$ and $(1 - m\alpha) < 0$ if $\alpha > \frac{1}{m}$.

Theorem 4.6. *Collision point L_0 is a:*

- Singularity of $\Omega_{\alpha,m}$ if $\alpha \leq -1$.
- Cuspidal point of $\Omega_{\alpha,m}$ if $-1 < \alpha < 0$, where the derivatives F_x and F_y are not defined.
- Peak of $\Omega_{\alpha,m}$ if $0 < \alpha < 1$, where the second derivatives F_{xx} , F_{xy} and F_{yy} are not defined.
- Minimum of $\Omega_{\alpha,m}$ if $1 < \alpha < \frac{1}{1-m}$.
- Saddle of $\Omega_{\alpha,m}$ if $\alpha > \frac{1}{1-m}$.

The extended Jacobi constant of L_0 is $J_0(\alpha, m) = (1 - m)\frac{2}{\alpha+1} + m^2$ for $\alpha > -1$.

In the results section 5.1.2 some surface images depicting the little difference between peaks and cuspidal points are depicted.

For the secondary collision, $L_{-1} = (m - 1, 0)$, the Hessian matrix of $\Omega_{\alpha,m}$ is the hessian matrix:

$$D^2\Omega_{\alpha,m}(L_{-1}) = \begin{pmatrix} 1 - (1 - m)\alpha & 0 \\ 0 & m \end{pmatrix} \quad (4.31)$$

Where $m > 0$ and $1 - (1 - m)\alpha > 0$ if $\alpha < \frac{1}{1-m}$ and $1 - (1 - m)\alpha < 0$ if $\alpha > \frac{1}{1-m}$.

Theorem 4.7. Collision point L_{-1} is a:

- Singularity of $\Omega_{\alpha,m}$ if $\alpha \leq -1$.
- Cuspidal point of $\Omega_{\alpha,m}$ if $-1 < \alpha < 0$, where the derivatives F_x and F_y .
- Peak of $\Omega_{\alpha,m}$ if $0 < \alpha < 1$, where the second derivatives F_{xx}, F_{xy} and F_{yy} are not defined.
- Minimum of $\Omega_{\alpha,m}$ if $1 < \alpha < \frac{1}{m}$.
- Saddle of $\Omega_{\alpha,m}$ if $\alpha > \frac{1}{m}$.

The extended Jacobi constant of L_0 is $J_0(\alpha, m) = (1 - m)\frac{2}{\alpha+1} + m^2$ for $\alpha > -1$.

4.8.3 Equilateral equilibrium points

Equilateral equilibrium points, $L_{4,5} = (m - \frac{1}{2}, \pm \frac{\sqrt{3}}{2})$, have Jacobi constant

$$J_{4,5}(\alpha, m) = 2\Omega_{\alpha,m}(L_{4,5}) = 1 - m(1 - m) \quad (4.32)$$

Hessian matrix $D^2\Omega_{\alpha,m}(L_{4,5})$ at these points is:

$$\begin{pmatrix} 1 - (1 - m)[1 + (\alpha - 1)\frac{1}{4}] - m[1 + (\alpha - 1)\frac{1}{4}] & \pm(1 - m)(\alpha - 1)\frac{\sqrt{3}}{4} \mp (\alpha - 1)\frac{\sqrt{3}}{4} \\ 1 - (1 - m)[1 + (\alpha - 1)\frac{3}{4}] - m[1 + (\alpha - 1)\frac{3}{4}] & \pm(1 - m)(\alpha - 1)\frac{\sqrt{3}}{4} \mp (\alpha - 1)\frac{\sqrt{3}}{4} \end{pmatrix} \quad (4.33)$$

Which is equivalent to

$$D^2\Omega_{\alpha,m}(L_{4,5}) = -\frac{\alpha - 1}{2} \begin{pmatrix} 1 & \mp\sqrt{3}(1 - 2m) \\ \mp\sqrt{3}(1 - 2m) & 3 \end{pmatrix} \quad (4.34)$$

The eigenvalues of this matrix are

$$\lambda_{\pm} = (1 - \alpha)(1 \pm \sqrt{1 - 3m + 3m^2}) = (1 - \alpha)(1 \pm \sqrt{3(m - \frac{1}{2})^2 + \frac{1}{4}}) \quad (4.35)$$

Which are positive for $\alpha < 1$ and negative for $\alpha > 1$ for $\forall m \in [0, 0.5]$.

Theorem 4.8. *Equilateral equilibrium points $L_{4,5}$ are:*

- Minimums of $\Omega_{\alpha,m}$ if $\alpha < 1$.
- Maximums of $\Omega_{\alpha,m}$ if $\alpha > 1$.

The extended Jacobi constant of $L_{4,5}$ is $J_{4,5} = 1 - m(1 - m)$.

4.8.4 Collinear equilibrium points

Collinear equilibrium points, $L_i = (a_i(\alpha, m) + m, 0)$, $i = 1, 2, 3$, have extended Jacobi constants:

$$J_i = 2\Omega_{\alpha,m}(L_i) = (1 - m)(a_i^2 - 2v_\alpha(|a_i|)) + m((a_i + 1)^2 - 2v_\alpha(|a_i + 1|)) - m(1 - m) \quad (4.36)$$

For $i = 1, 2, 3$ Hessian matrix, $D^2\Omega_{\alpha,m}(L_i)$, at these points is:

$$\begin{pmatrix} 1 - (1 - m)\alpha|a_i|^{\alpha-1} - m\alpha|a_i + 1|^{\alpha-1} & 0 \\ 0 & 1 - (1 - m)|a_i|^{\alpha-1} - m|a_i + 1|^{\alpha-1} \end{pmatrix} \quad (4.37)$$

The eigenvalues of this matrix are:

$$\lambda_1 = 1 - (1 - m)\alpha|a_i|^{\alpha-1} - m\alpha|a_i + 1|^{\alpha-1} \quad (4.38)$$

$$\lambda_2 = 1 - (1 - m)|a_i|^{\alpha-1} - m|a_i + 1|^{\alpha-1} \quad (4.39)$$

The collinear equilibrium equation

$$x_i - (1 - m)(x_i - m)|a_i|^{\alpha-1} - m(x_i - m + 1)|a_i + 1|^{\alpha-1} = 0 \quad (4.40)$$

can be rewritten as

$$x_i(1 - (1 - m)|a_i|^{\alpha-1} - m|a_i + 1|^{\alpha-1}) + m(1 - m)(|a_i|^{\alpha-1} - |a_i + 1|^{\alpha-1}) = 0 \quad (4.41)$$

Let $\zeta_i = (1 - m)|a_i| + m|a_i + 1|$ be considered. Then the second eigenvalue is equivalent to the following expression:

$$\zeta_i - 1 = \frac{m(1 - m)}{x_i}(|a_i|^{\alpha-1} - |a_i + 1|^{\alpha-1}) \quad (4.42)$$

- For L_1 , $|a_i| < 1$ and $|a_{i+1}| < 1$. Therefore, $\zeta_i > 1$ for $\alpha < 1$ and $\zeta_i < 1$ for $\alpha > 1$.

- For L_2 , $x_i = a_i + m < 0$ and $|a_i| < |a_{i+1}|$. Therefore, $\zeta_i > 1$ for $\alpha < 1$ and $\zeta_i < 1$ for $\alpha > 1$.
- For L_3 , $x_i = a_i + m < 0$ and $|a_i| < |a_{i+1}|$. Therefore, $\zeta_i > 1$ for $\alpha < 1$ and $\zeta_i < 1$ for $\alpha > 1$.

From which one can conclude that the first eigenvalue is positive for $\alpha < 1$ and negative for $\alpha > 1$.

Theorem 4.9. *The collinear equilibrium points L_i , $i = 1, 2, 3$, are: Saddles of $\Omega_{\alpha,m}$ if $\alpha < 1$ or $\alpha > 1$. For the case $\alpha < 1$ the unstable varieties follow the $x - axis$ direction and the stable varieties follow the $y - axes$ direction. For the case $\alpha > 1$ the unstable and stable directions are exchanged.*

4.8.5 Coincidences of extended Jacobi constants

The idea is to study zero-velocity curves in terms of extended Jacobi constants ordering. Extended Jacobi constants at equilateral equilibrium points, $J_{4,5}$, coincide for all values of α .

In this section we are going to study some other coincidences which are also important. Since coincidences are where the ordering changes take place. The ordering changes will be discussed in section 4.8.6.

- Case $\alpha = 0$.

Extended Jacobi constants of collinear equilibrium points coincide when $\alpha = 0$. Thus, their extended Jacobi constants coincide as well:

$$J_i(0, m) = 0, i = 0, 1, 2, 3 \quad (4.43)$$

- Case $\alpha = \bar{\alpha}(m)$.

Jacobi constants $J_3(\alpha, m)$ and $J_{-1}(\alpha, m)$ coincide at a value $\alpha = \bar{\alpha}(m)$.

- Case $\alpha = 1$.

For the case $\alpha = 1$ Jacobi constants of all the critical points coincide and are:

$$J_i(0, m) = 1 - m(1 - m), i = -1 \div 5 \quad (4.44)$$

- Case $\alpha = \frac{1}{1-m}$ and $\alpha = \frac{1}{m}$.

As collinear equilibrium points $L_1(\alpha, m)$, $L_2(\alpha, m)$ and $L_{-1}(m) = (m-1, 0)$ coincide when $\alpha = \frac{1}{1-m}$. Therefore their Jacobi constants also do:

$$J_1\left(\frac{1}{m-1}, m\right) = J_2\left(\frac{1}{m-1}, m\right) = J_{-1}\left(\frac{1}{m-1}, m\right) = -\frac{m(1-m)^2}{2-m} \quad (4.45)$$

The equation of a_1 is

$$a_1 + m + (1-m)(-a_1^\alpha - m(a_1+1)^\alpha) = 0 \quad (4.46)$$

Let the equation $a_1 = -1 + b_1$ for $\alpha < 1$ be considered:

$$-1 + b_1 + m(1-m)(-1 + b_1)^\alpha - m(b_1)^\alpha = 0 \quad (4.47)$$

which can be written

$$b_1(1 + (1-m)\frac{(1-b_1)^\alpha - 1}{b_1} - mb_1^{\alpha-1}) = 0 \quad (4.48)$$

The equation of a_2 is

$$a_2 + m + (1-m)(-a_2^\alpha - m(a_2+1)^\alpha) = 0 \quad (4.49)$$

Let the equation $a_2 = -1 + b_2$ for $\alpha > 1$ be considered:

$$-1 + b_2 + m(1-m)(-1 + b_2)^\alpha - m(b_2)^\alpha = 0 \quad (4.50)$$

which can be written as

$$b_2(1 + (1-m)\frac{(1-b_2)^\alpha - 1}{b_2} - mb_2^{\alpha-1}) = 0 \quad (4.51)$$

The second factor tends to $1 - (1-m)\alpha$ and it vanishes for $\alpha = \frac{1}{1-m}$, which indicates the coincidence of L_1 and L_2 with L_{-1} when $\alpha = \frac{1}{1-m}$.

The other collinear equilibrium, $L_3(\alpha, m)$, coincides with the collision equilibrium $L_0(\alpha, m)$. They coincide when $\alpha = \frac{1}{m}$. Their extended Jacobi constant is:

$$J_3\left(\frac{1}{m-1}, m\right) = J_0\left(\frac{1}{m-1}, m\right) \quad (4.52)$$

The equation of a_3 for $\alpha > 1$

$$a_3 + m - (1-m)a_3^\alpha - m(a_3+1)^\alpha = 0 \quad (4.53)$$

can be written as

$$a_3(1 - m\frac{a_3^\alpha - 1}{a_3} - (1-m)a_3^{\alpha-1}) = 0 \quad (4.54)$$

The second factor tends to $1 - m\alpha$ and it vanishes for $\frac{1}{m}$, which indicates the coincidence of L_3 and L_0 when $\alpha = \frac{1}{m}$.

4.8.6 Extended Jacobi constants ordering

Given the mass parameter m , the ordering of extended Jacobi constants varies depending on the α parameter. The following lines are devoted to present the ordering of extended Jacobi constants at the critical points of $\Omega_{\alpha,m}$ depending on different α intervals.

In this section the dependence on α, m of the extended Jacobi constants has been omitted in order to ease the notation.

For $\alpha < -1$ extended Jacobi constants ordering is $J_{4,5} < J_3 < J_2 < J_1$.

For $-1 < \alpha < 0$ extended Jacobi constants ordering is $J_{4,5} < J_3 < J_2 < J_1 < J_{-1} < J_0$.

For $\alpha = 0$ extended Jacobi constants of the collinear equilibrium points J_3, J_2, J_1 coincide and take value $1 + m^2$. Before this coincidence the ordering of the constants is $J_{4,5} < J_3 < J_2 < J_1 < J_{-1} < J_0$ and afterwards it is $J_{4,5} < J_1 < J_2 < J_3 < J_{-1} < J_0$. After this coincidence the ordering of J_3, J_2, J_1 has been exchanged.

For $0 < \alpha = \bar{\alpha}(m) < 1$ constants J_3, J_{-1} coincide. Before this coincidence the ordering of these two constants is $J_3 < J_{-1}$ and afterwards it comes to be exchanged $J_{-1} < J_3$.

For $\alpha = 1$ all extended Jacobi constants coincide and take value $J_i = 1 - m(1 - m)$ for $i = 1, 2, \dots, 5$. Before this coincidence the ordering is $J_{4,5} < J_1 < J_2 < J_{-1} < J_3 < J_0$ and afterwards it results in $J_0 < J_3 < J_{-1} < J_2 < J_1 < J_{4,5}$. We can see the ordering has been reversed.

For $\alpha = \frac{1}{1-m}$ extended Jacobi constants of collinear equilibrium points L_1, L_2 coincide with collision point L_{-1} . They take value $-\frac{m(1-m)^2}{2-m}$. After this coincidence the constant ordering remains $J_0 < J_3 < J_{-1} < J_{4,5}$.

For $\alpha = \frac{1}{m}$ collinear equilibrium point L_3 coincides with collision equilibrium point L_0 . After this coincidence L_3 passes to equilibrium point L_1 . Therefore Jacobi constant ordering at $\alpha = \frac{1}{m}$ is $J_1 = J_3 = J_0 < J_3 < J_{-1} < J_{4,5}$ and afterwards it is $J_1 < J_0 < J_{-1} < J_{4,5}$. Where it can be observed that the ordering of the two first constants has been exchanged.

Figure 4.2 depicts the bifurcation in α of the colinear equilibrium points abscissae and the extended Jacobi constants of all the characteristic points for $\alpha \in [-2, 6]$ for the particular case with $m = 0.25$. It can be observed that the orderings match with the ones discussed previously and summarized in table 4.8.5. Changes in the mass parameter would change the graphics but not the bifurcation diagram nor the orderings.

In table 4.2 all the previously discussed information is summarized.

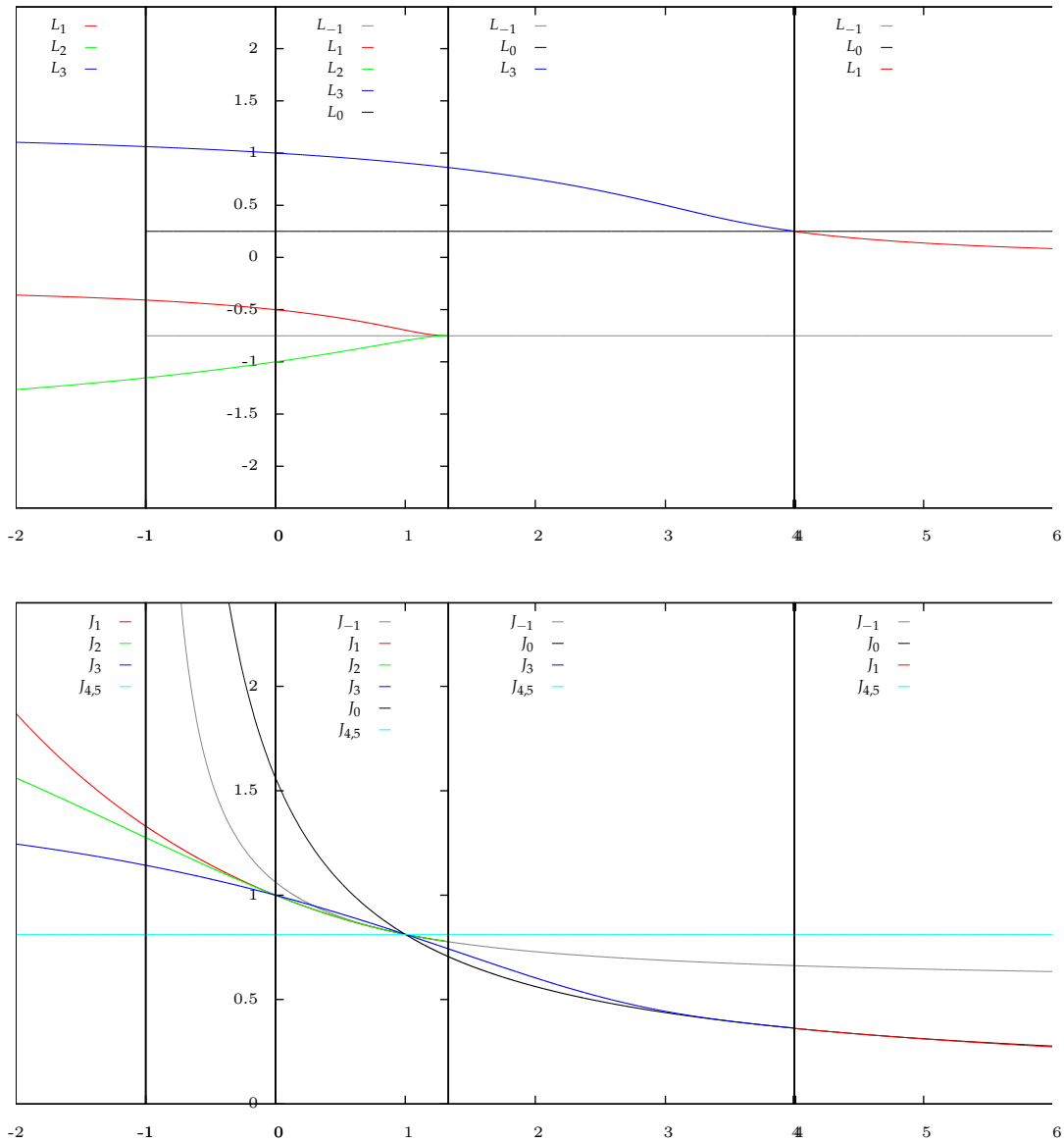


Figure 4.2: $m = 0.25$: collinear equilibria abscissae and extended Jacobi constants of all the characteristic points for $\alpha \in [-2, 6]$. Observe the ordering changes for $\alpha = -1, 0, 1, \frac{4}{3}, 4$.

Table 4.2: Extended Jacobi constants orderings

α intervals	Jacobi constants ordering
$\alpha < 1$	$J_{4,5} < J_3 < J_2 < J_1$
$-1 < \alpha < 0$	$J_{4,5} < J_3 < J_2 < J_1 < J_{-1} < J_0$
$\alpha = 0$	$J_{4,5} < J_1 = J_2 = J_3 = 1 < J_{-1} = 1 + m^2 < J_0 = 1 + (1 - m)^2$
$0 < \alpha < \bar{\alpha}(m)$	$J_{4,5} < J_1 < J_2 < J_3 < J_{-1} < J_0$
$\alpha = \bar{\alpha}(m)$	$J_{4,5} < J_1 < J_2 < J_3 = J_{-1} < J_0$
$\bar{\alpha}(m) < 1$	$J_{4,5} < J_1 < J_2 < J_{-1} < J_3 < J_0$
$\alpha = 1$	$J_i = 1 - m(1 - m), i = 1 \div 5$
$1 < \alpha < \frac{1}{1-m}$	$J_0 < J_3 < J_{-1} < J_2 < J_1 < J_{4,5}$
$\alpha = \frac{1}{1-m}$	$J_0 < J_3 < J_{-1} = J_2 = J_1 = -\frac{m(1-m)^2}{2-m} < J_{4,5}$
$\frac{1}{1-m} < \alpha < \frac{1}{m}$	$J_0 < J_3 < J_{-1} < J_{4,5}$
$\alpha = \frac{1}{m}$	$J_1 = J_3 = J_0 < J_3 < J_{-1} < J_{4,5}$
$\frac{1}{m} < \alpha$	$J_1 < J_0 < J_{-1} < J_{4,5}$

4.8.7 Bifurcation diagrams of the extended Jacobi function

In section 4.8.1 a study of $\Omega_{\alpha,m}$ critical points and their local stability has been performed. Critical points have been classified into minimum, maximum and saddle points. These points are of great interest in this study because they are the places where births, deaths and behaviour changes of level curves take place.

In section 4.8.5 extended Jacobi constants coincidences at characteristic points have been studied. Finally, the orderings of these constants depending on α parameter have been discussed in section 4.8.6.

In this section all this previously studied information is summarized into bifurcation diagrams depending on α parameter intervals. This diagrams will be of great value when dealing with information computation near critical points.

These bifurcation diagrams are the bifurcation diagrams that will be implemented in the 3-body problem code. A different function of code will be used for each of the following α intervals.

Each of the following tables indicate the ordering of the extended Jacobi constants from left to right. For each constant, the table shows the kind of critical point of the surface and either it is birth, a death a split or a merge. The curves associated to each part is also indicated.

In order to ease the notation, the index j of $C[j][k]$ has been omitted in order to denote the curves $C_0, C_1, C_2...$ in each part j .

Table 4.3: Bifurcation diagram for case $\alpha < -1$

$J_{4,5}$	J_3	J_2	J_1	$J_{-1} = J_0 = \infty$
minimum	saddle	saddle	saddle	singular
birth	merge	split	split	...
C_0, C_1	C_0	C_0, C_1	C_0, C_1, C_2	\rightarrow

Table 4.4: Bifurcation diagram for case $-1 < \alpha < 0$

$J_{4,5}$	J_3	J_2	J_1	J_{-1}	J_0
minimum	saddle	saddle	saddle	cuspid	cuspid
birth	merge	split	split	death	death
C_0, C_1	C_0	C_0, C_1	C_0, C_1, C_2	C_0, C_1	$C_0 \rightarrow$

Table 4.5: Bifurcation diagram for case $0 < \alpha < \bar{\alpha}(m)$

$J_{4,5}$	J_1	J_2	J_3	J_{-1}	J_0
minimum	saddle	saddle	saddle	maximum	maximum
birth	merge	split	split	death	death
C_0, C_1	C_0	C_0, C_1	C_0, C_1, C_2	C_0, C_1	$C_0 \rightarrow$

Table 4.6: Bifurcation diagram for case $\bar{\alpha}(m) < \alpha < 1$

$J_{4,5}$	J_1	J_2	J_{-1}	J_3	J_0
minimum	saddle	saddle	maximum	saddle	maximum
birth	merge	split	death	split	death
C_0, C_1	C_0	C_0, C_1	C_0	C_0, C_1	$C_0 \rightarrow$

Table 4.7: Bifurcation diagram for case $1 < \alpha < \frac{1}{1-m}$, reverse trace

J_0	J_3	J_{-1}	$J_{4,5}$
minimum	saddle	saddle	maximum
death	split	merge	birth
$\leftarrow C_0$	C_0, C_1	C_0	C_0, C_1

Table 4.8: Bifurcation diagram for case $\frac{1}{1-m} < \alpha < \frac{1}{m}$, reverse trace

J_0	J_3	J_{-1}	$J_{4,5}$
minimum	saddle	saddle	maximum
death	split	merge	birth
$\leftarrow C_0$	C_0, C_1	C_0	C_0, C_1

Table 4.9: Bifurcation diagram for case $\frac{1}{m} < \alpha$, reverse trace

J_0	J_{-1}	J_1	$J_{4,5}$
minimum	saddle	saddle	maximum
death	split	merge	birth
$\leftarrow C_0$	C_0, C_1	C_0	C_0, C_1

4.9 Bifurcation diagrams implementation

This section is dedicated to explaining the code lines related to the implementation of the bifurcation diagrams in α associated to the XPCR3BP. LC_XR3BP is the file that contains the following information.

Table 4.2 summarizes the information related to extended Jacobi constants orderings. It can be observed that there are seven different intervals of α in which the orderings of the constants do not change. The code has been organized following these seven intervals. For each one of them, a different function has been implemented. These functions contain the information related to the bifurcation diagrams in z which is summarized in the tables of section 4.8.7.

Figure 4.3 contains the code lines where the appropriated function is chosen in function of the α parameter chosen by the user. The AppInit function must be seen as the specific problem application which has been organized in seven different cases for the bifurcations in α . For simpler examples, such as the one discussed in section 1.2, the AppInit would only contain one bifurcation diagram in z .

```

void
AppInit()
{
    if (alpha <= -1)
        AppInitn();
    else if( alpha < 0 )
        AppInit0();
    else if (alpha <= 1) {
        double a3 = L3();
        double J3 = F0(a3 + m, 0);
        double Js = F0(-1 + m, 0);
        if (J3 < Js)
            AppInit11();
        else
            AppInit12();
    }
    else if( alpha < 1/(1-m) )
        AppInit21r();
    else if (alpha < 1/m )
        AppInit22r();
    else
        AppInit23r();
}

```

Figure 4.3: Code lines with the function that chooses the proper Init application depending on α . There are seven different applications, one for each α interval.

Let the function of the gravitational case function, $\alpha = -2$, be explained. Table 4.3 summarizes the information which is implemented in the code for the case $\alpha < -1$. Figures A.1, A.2, A.3 and A.4 show the different applications related to this specific case. The $[z_m, z_M]$ interval bifurcation diagram has been implemented in these code lines. The interval has been split in four different intervals. Each figure shows the code for each subinterval.

See appendix B where the evolution of zero-velocity curves for the classic gravitational case, $\alpha = -2$, is explained. This section may help understanding the code lines related to the gravitational problem.

4.10 Surface visualization of zero-velocity curves

All of the necessary theoretical background related to the XPCR3BP has been detailed in previous sections. The following step involves the implementation of the code for each α intervals detailed in section 4.8.6 with all the information collected in the bifurcation diagrams of section 4.8.7.

The surfaces to be represented are those associated to the functions $\Omega_{\alpha,m}$. The steps to be followed are the ones detailed for a general function F in sections 2 and 3. In this case the level curves are the zero-velocity curves for each extended Jacobi constant associated.

Chapter 5

Results and conclusions

5.1 Results

5.1.1 Simulator

The result of this project is a simulator that plots surfaces via level curves. The simulator has been specifically adapted for the XPCR3BP problem where zero-velocity curves are seen as level curves of the surface.

Figure 5.1 shows the appearance of the simulator interface.

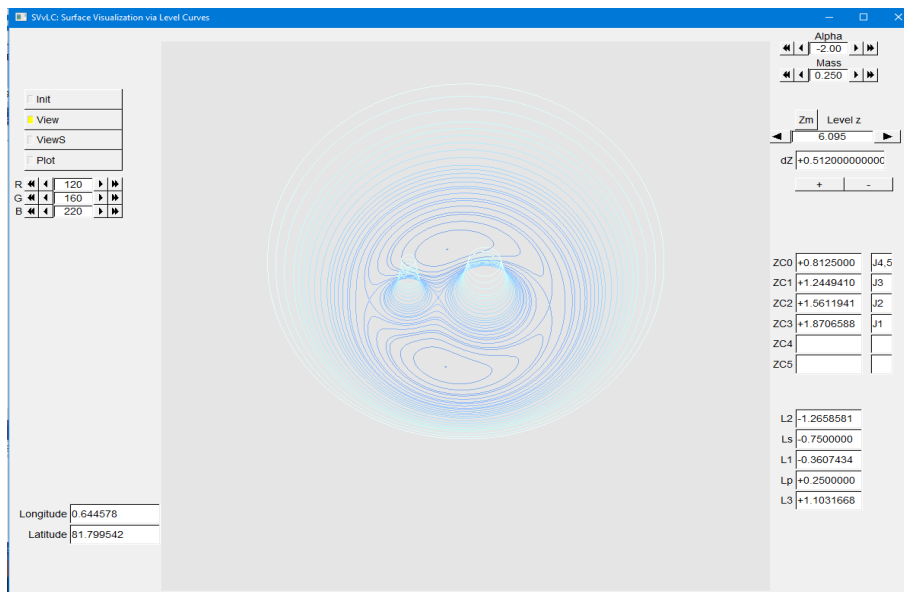


Figure 5.1: Simulator interface with zero-velocity surfaces for $m = 0.25$, $\alpha = -2$ (gravitational case).

Aside from the visual surface information, other important data can be accessed in the simulator.

On the right hand side, the information related to the specific problem is found: the α parameter, the mass parameter, the current z level and the dz increment. It also shows the levels at which curves appear. For each curve, on the right hand side, the corresponding extended Jacobi constant is detailed. In this way the results can be easily compared with the previous analytic study. The collinear equilibrium points x coordinate is also specified.

On the left hand side, the information related to the visualization simulator is shown: the different functions of the application, the RGB colour chosen and the latitude and longitude.

Let the different controls be explained.

On the right hand side the controls are:

- A control for changing the mass and another one for changing the α parameter.
- A control to change the dz increment and another one to move along the trace. This control must be used from low levels to high levels as the simulator does not erase the already displayed levels. Next to these two controls there is a button that moves z to the lowest level which must be used when the mass and α parameters have been changed.

On the left hand side the controls are:

- Buttons to choose the function of the simulation:
 - Init: This function displays only the level curves at the current level z . As the level moves, new curves appear and the previous ones do not appear anymore.
 - View: This function displays the level curves of each level z at their corresponding level. It is useful to grasp the surface appearance and see as well the level curves.
 - ViewS: This function displays the surface as the level z increases.
 - Plot: This function collects the computed points to a .out file. This function must be used when representing gnuplot 2-D graphic of the level curves.
- An RGB control that enables the user change the colour of the surface.

5.1.2 Surfaces depending on the α interval

In this section some of the graphic results of the simulation will be discussed. Five different cases depending on α . Values of α in different intervals have been chosen. All of the images that are discussed in this section have been computed for $m = 0,25$, as the changes in m do not affect the extended Jacobi constants orderings.

For each case, three different images are shown. Firstly, the 2D representation of zero-velocity curves obtained with gnuplot appears. This graph is useful to see more precisely the singular curves. Secondly, two 3D images of the simulator are shown: one with the surface and another with the level curves for each level z .

- Case $\alpha = -2 < -1$ (see fig. B.1, fig. B.2), which corresponds to the 1st interval discussed in section 4.8.6. This is the classical gravitational problem. In table 4.2 the ordering of extended Jacobi constants is $J_{4,5} < J_3 < J_2 < J_1$, which coincides with the ordering in the simulator screen in figure B.2. This case is interesting because there are singularities at the primary and the secondary bodies.
- Case $\alpha = -0.50 \in (-1, 0)$ (see fig. B.3, fig. B.4), which corresponds to the 2nd interval discussed in section 4.8.6. In table 4.2 the ordering of extended Jacobi constants is $J_{4,5} < J_3 < J_2 < J_1 < J_{-1} < J_0$, which coincides with the ordering in the simulator screen in figure B.4. This case is interesting because a cuspidal point can be seen at the primary and secondary bodies where the derivative of the tangent field is unbounded.
- Case $\alpha = 0.50 \in (\bar{\alpha}(m), 1)$ (see fig. B.5, fig. B.6), which corresponds to the 4th interval discussed in section 4.8.6. In table 4.2 the ordering of extended Jacobi constants is $J_{4,5} < J_1 < J_2 < J_{-1} < J_3 < J_0$, which coincides with the ordering in the simulator screen in figure B.6. In this case peak points where the second derivatives of the tangent field are unbounded appear. The cuspidal points that appear at B.4 do not appear anymore. Instead, in figure B.6, maximums appear at the primary and secondary bodies.
- Case $\alpha = 1.50 \in (\frac{1}{1-m}, \frac{1}{m})$ (see fig. B.7, fig. B.8), which corresponds to the 6th interval discussed in section 4.8.6. This case has been displayed with the reverse trace. Therefore the z -axis is seen upside-down. In table 4.2 the ordering of extended Jacobi constants is $J_0 < J_3 < J_{-1} < J_{4,5}$, which coincides with the ordering in the simulator screen in figure B.8.
- Case $\alpha = 6 > \frac{1}{m}$ (see fig. B.9, fig. B.10), which corresponds to the 7th interval discussed in section 4.8.6. This case has been displayed with the reverse

trace. Therefore the z-axis is seen upside-down. In table 4.2 the ordering of extended Jacobi constants is $J_1 < J_0 < J_{-1} < J_{4,5}$, which coincides with the ordering in the simulator screen in figure B.10.

5.2 Conclusions

In this section the conclusions of this project are presented.

The general program implementation has come as a result of the need for a surface visualisation application. At first, the intention of this project was to include all the information related to the specific application in one same code modulus. In this way the simulator can be easily adapted to many different problems by changing only one of the code files. The modulus `LC_XR3BP.cpp` is the file with the code source related to the XPCR3BP. However, the modulus `LC_Compute.cpp` does also contain specific information such as the tangent field. The ideal situation would have been to avoid the tangent field information in this file. Nevertheless, these code lines can be easily changed for other applications. It is also important to remark that in the XPCR3BP most of the programming efforts have been made in the specific modulus. `LC_XR3BP.cpp` contains a different function for each interval of α previously discussed in section 4.8.6. For the simple example given in section 1.2 the specific modulus does only contain one function as there are no parameter dependencies.

The XPCR3BP problem has been of great interest in this surface representation problem. The most natural case of study for this problem is the classical gravitational problem where $\alpha = -2$. The extended problem, where α may take other values does not make physical sense. However, the implementation of the extended problem has produced more complex surfaces for this study. Therefore, the implementation of the XPCR3BP code has been more complicated. For example, at the beginning of this project the surface was not displayed properly near complicated points such as peaks and cuspids. This problem this problem occurred due to the fact that in such points the field is too big or its first or second derivatives whether disappear or are unbounded. These problems has required more than one change of the code in order to visualize the surface near these points.

One of the difficulties found in these problem has been that, for certain α values, some extended Jacobi constants are very close to one another. This fact makes the problem more difficult and more work has to be done.

In certain figures in appendix B, some little wholes of the surface can be observed. This problem has been refined in this project. However, in future works

the code could be even more refined with the intention to cover up all the surface.

For future works, non simple closed curves could be taken into account. In such a case, the condition for stopping the integration of level curves must be changed. In this project the numerical integration stops when the cutting line is cut following the same direction as the one followed in the cutting point. When dealing with curves that prolong till infinite, other criteria for stopping should be implemented.

The other simplification that has been taken into consideration in this project is that critical level curves at saddle points are meant to be homoclinic. For future works, this restriction can also be ignored and heteroclinic curves can be included. In this case the criteria for stopping the integration of such points must be also adapted. In the bifurcation diagram some new information about these heteroclinic curves may have to be included.

Another extension of this project could be to adapt this program to the case where level sets are surfaces instead of being curves. For this case, other physical problems can be visualized with the application. For example, the visualization of the hydrogen atom orbitals.

section

Appendix A

The classical problem

A Classical problem Jacobi constants

In the case of gravitational forces, with $\alpha = -2$, the extended Jacobi constant is

$$J(-2, m) = (1 - m)(r_1^2 - 2(-r_1^{-1} - 1)) + m(r_2^2 - 2(-r_2^{-1} - 1)) - m(1 - m) = C(m) - 2 \quad (\text{A.1})$$

where

$$C(m) := (1 - m)(r_1^2 + \frac{2}{r_1}) + m(r_2^2 + \frac{2}{r_2} - m(1 - m)) \quad (\text{A.2})$$

is the gravitational Jacobi integral. The constant -2 in the expression appears as result of the potential origin chosen.

The extended Jacobi constants for each equilibrium point of the classical problem are:

- Collinear equilibrium points, $L_i(-2, m) = (a_i(-1, m) + m, 0)$, $i = 1, 2, 3$, have the extended Jacobi constants

$$J_i(-2, m) = (1 - m)(a_i^2 + 2(\frac{1}{a_i} - 1)) + m((a_i + 1)^2 + 2(\frac{1}{(a_i + 1)^2} - 1)) - m(1 - m) = C_i(m) - 2 \quad (\text{A.3})$$

- Equilateral equilibrium points, $L_i(-2, m) = (m - \frac{1}{2}, \frac{\sqrt{3}}{2})$, $i = 4, 5$, have extended Jacobi constants

$$J_i(-2, m) = 1 - m(1 - m) = C_i(m) - 2 \quad (\text{A.4})$$

B Zero-velocity curves description for the classical problem

In this appendix section the zero-velocity curves for the case $\alpha = -2$ are detailed.

The zero-velocity curves appear around the two points in L_4 and L_5 from the corresponding value $C_{4,5} = 3 - m(1 - m)$ for increasing values of C .

For increasing values of C between $C_{4,5}$ and $C_3(m)$ these two closed zero-velocity curves grow as two separated components around L_4 and L_5 . These curves encircle two prohibited regions which are symmetrically disposed with respect to the x -axis. These two curves match at L_3 beyond the primary body.

For increasing values of C between $C_3(m)$ and $C_2(m)$ the closed zero-velocity curve continues growing and surrounding the prohibited region. This region contains L_3, L_4 and L_5 . The curve folds by touching itself at L_2 beyond the secondary body.

For increasing values of C between $C_2(m)$ and $C_1(m)$, there are two closed zero-velocity curves. The outer one continues growing and allows outer movements. The inner one continues reducing and allows movements in the inner region which contains the primary and the secondary bodies. This inner curve touches itself at L_1 between the primary and the secondary body and splits afterwards.

For increasing values of C beyond the value $C_1(m)$, the outer zero-velocity closed curve continues growing. It allows outer movements. The two split inner zero-velocity curves continue reducing. They allow movements near the primary body or near the secondary body.

C Program code for the case $\alpha < -1$

In this appendix section some images of code lines for the case $\alpha < -1$ are detailed. As it has been explained in previous sections, the function `AppInit` contains the information related to the bifurcation in α of the XPCR3BP. It is the one responsible for the specific function chosen depending on the α parameter chosen. The following images contain the bifurcation diagram in z associated to the first interval of α . For each interval of α a different application has been programmed. Each one of the other applications are not detailed in this section but they follow the same structure as these one but attending the proper bifurcation diagrams found in section 4.8.7.

These code lines are associated to the level curves evolution for $\alpha < -1$. In order to understand more easily the description given, see figure B.1 and figure

B.2 which correspond to the gravitational case $\alpha = -2$.

```

TWO MINIMA at L4 and L5 at same level J4=J5
BIRTH - 2 curves C0, C1 are born surrounding L4, L5,
with line cuts at  $y_0 = \pm \sqrt{3}/2$ 
C0(L4), C1(L5)
ZC[0] = 1 - m * (1 - m);
JC[0] = "J4,5";
Zx0[0] = vector<double>(2);
Zy0[0] = vector<double>(2);
Zy0[0][0] = sqrt(3.) / 2;
Zx0[0][0] = m - 0.5;
Zy0[0][1] = -sqrt(3.) / 2;
Zx0[0][1] = m - 0.5;
F2(-0.5 + m, sqrt(3.) / 2, F, Fx, Fy, Fxx, Fxy, Fyy);
eigen(Fxx, Fxy, Fyy, 1, vx, vy);
Zvx[0] = vector<double>(2);
Zvy[0] = vector<double>(2);
Zk[0] = vector<int>(2);
Zvx[0][0] = -1;
Zvy[0][0] = vy;
Zvx[0][1] = -1;
Zvy[0][1] = vy;
Zk[0][0] = -1;
Zk[0][1] = -1;
ZLS[0] = vector<vector<double>>(2);

```

Figure A.1: Code lines for the case $\alpha < -1$ for the birth of two curves C_0, C_1 which appear at the same level surrounding L_4 and L_5 respectively. These curves correspond to two different minimums which are symmetrically disposed with respect to the x -axis. $ZC[0]$, which contains the critical level, and $JC[0]$, which contains the name of the extended Jacobi constants. The cutting line for C_0 is saved in $Zy0[0][0] = \sqrt{\frac{3}{2}}$ and the cutting line for C_1 is saved in $Zy0[0][1] = -\sqrt{\frac{3}{2}}$. The function `eigen` is related to the stability study of the critical points. It is related to the eigenvalues and eigenvectors (for saddles) of the tangent field derivative. It saves vx and vy directions treating separately saddle points from minimums and maximums. $Zvx[0][0]$ and $Zvx[0][1]$ are initialized at -1 as there are two minimums (for cusps, this number would be -2 ; for saddles, the unstable direction would be saved). The vector Zk contains the information about the curves continuation where -1 stands for a curve that does not continue. $ZLS[0]$ is declared with two components as there are two curves. In all the vectors the index 0 stands for the first interval of the $[z_m, z_M]$ partition in each vector.

```

SADDLE at L3
MERGE - the 2 curves C0, C1 collide at L3 and
merge in one curve with line cuts at y0=0
C0(L4, L3, L5)
a3 = L3();
ZC[1] = F0(a3 + m, 0);
JC[1] = "J3";
Zy0[1] = vector<double>(1);
Zx0[1] = vector<double>(1);
Zy0[1][0] = 0;
Zx0[1][0] = a3 + m;
Zvx[1] = vector<double>(1);
Zvy[1] = vector<double>(1);
Zk[1] = vector<int>(1);
F2(a3 + m, 0, F, Fx, Fy, Fxx, Fxy, Fyy);
eigen(Fxx, Fxy, Fyy, l, vx, vy);
Zvx[1][0] = vx;
Zvy[1][0] = vy;
Zk[1][0] = -1;
ZLS[1] = vector<vector<double>>(1);

```

Figure A.2: Code lines for the case $\alpha < -1$ for the saddle point at L_3 where there is a saddle point. The curves C_0 and C_1 collide and merge into a single one, C_0 . In this interval there is a merge, therefore, all the vectors in these code lines have only one component. The cutting line for C_0 is saved in $Zy0[1][0] = 0$. As there is a saddle point at L_3 , $Zvx[1][0] = vx$ and $Zvy[1][0] = vy$. $Zk[1][0] = -1$ as the curve does not continue. $ZLS[1]$ has one component as there is only one curve. The index 1 stands for the second interval of the $[z_m, z_M]$ partition.

```

SADDLE at L2
SPLIT- the curve C0 folds and autocollides
left at L2 and splits in two curves:
outer C0 and inner C1 crossing m1 and m2
with line cuts at y0=0
C0(L4, L2, L3, L5), C1(m2, L1, m1)
a2 = L2();
ZC[2] = F0(a2 + m, 0);
JC[2] = "J2";
Zy0[2] = vector<double>(2);
Zx0[2] = vector<double>(2);
Zy0[2][0] = 0;
Zx0[2][0] = a2 + m;
Zy0[2][1] = 0;
Zx0[2][1] = a2 + m;
Zvx[2] = vector<double>(2);
Zvy[2] = vector<double>(2);
Zk[2] = vector<int>(2);
F2(a2 + m, 0, F, Fx, Fy, Fxx, Fxy, Fyy);
eigen(Fxx, Fxy, Fyy, 1, vx, vy);
Zvx[2][0] = -vx;
Zvy[2][0] = -vy;
Zvx[2][1] = vx;
Zvy[2][1] = vy;
Zk[2][0] = 0;
Zk[2][1] = -1;
ZLS[2] = vector<vector<double>>(2);

```

Figure A.3: Code lines for the case $\alpha < -1$ for the saddle point at L_2 where the curve C_0 splits in two curves: C_0 is the outer one and C_1 . C_0 encloses L_4, L_2, L_3 and L_5 while C_1 is the inner one and encloses L_1 , the primary and the secondary bodies. In this interval there is a split, therefore, all the vectors in these code have two components again. See that the two cutting lines do not coincide anymore but now $Zx0[2][0] = Zx0[2][1] = a2 + m$. As there is a saddle point at L_2 , the unstable directions are saved for each curve. $Zk[2][0] = 0$ as this curve continues in the following part. $Zk[2][1] = -1$ as C_1 does not continue.

```

SADDLE at L1
SPLIT: curve C0 follows and C1 autocollides
center at L1 and splits in two curves:
- C1 and C2 crossing m1 and m2 with line cuts at y0=
C0(L4, L2, L1, L3, L5), C1(m1), C2(m2)
a1 = L1();
ZC[3] = F0(a1 + m, 0);
JC[3] = "J1";
Zy0[3] = vector<double>(3);
Zx0[3] = vector<double>(3);
Zy0[3][0] = 0;
Zx0[3][0] = 0;
Zy0[3][1] = 0;
Zx0[3][1] = a1 + m;
Zy0[3][2] = 0;
Zx0[3][2] = a1 + m;
F2(a1 + m, 0, F, Fx, Fy, Fxx, Fxy, Fyy);
eigen(Fxx, Fxy, Fyy, l, vx, vy);
Zvx[3][0] = 0;
Zvy[3][0] = 0;
Zvx[3][1] = -vx;
Zvy[3][1] = -vy;
Zvx[3][2] = vx;
Zvy[3][2] = vy;
Zk[3][0] = -1;
Zk[3][1] = -1;
Zk[3][2] = -1;
ZLS[3] = vector<vector<double>>(3):

```

Figure A.4: Code lines for the case $\alpha < -1$ for the saddle point at L_1 where the curve C_0 continues and encloses L_4, L_2, L_3 and L_5 . The curve C_1 splits in two curves: C_1 and C_2 which enclose the primary and the secondary bodies respectively. As C_0 continues and there is a saddle point with a split at L_1 , all the vectors in this code lines have 3 components as there are 3 curves. $Zk[3][0] = Zk[3][1] = Zk[3][2] = -1$ as the three curves do not continue as this interval is the last one.

Appendix B

Resulting images

This appendix section contains some of the visualizations obtained with the simulator for different values of α . For each case, three different images are shown. Firstly, the 2D plot of the zero-velocity curves. Secondly, the 3D surface obtained is showed. Finally, the 3D representation of the level curves associated to the surface can be found. In the three different representations the darkest blue indicates the lowest levels and the colour brightens for higher z levels.

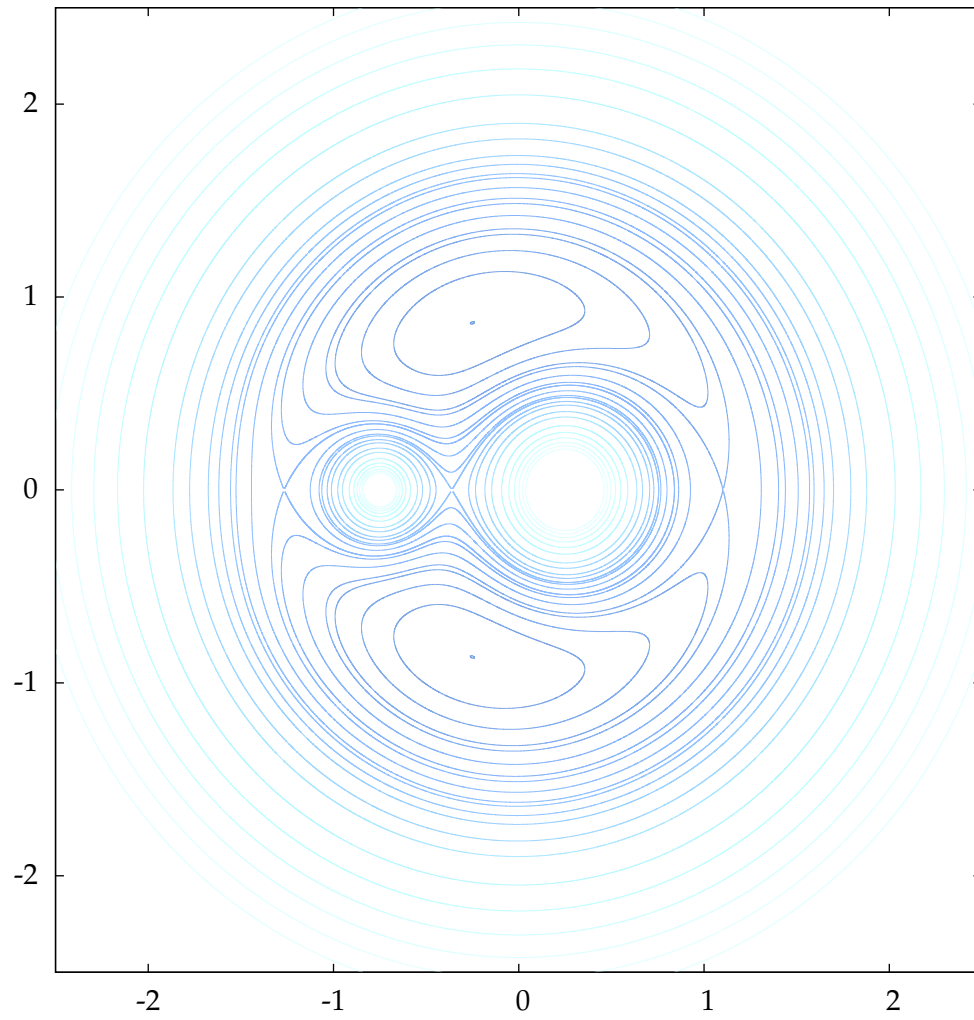


Figure B.1: Zero-velocity curves for $m = 0.25$, $\alpha = -2$.

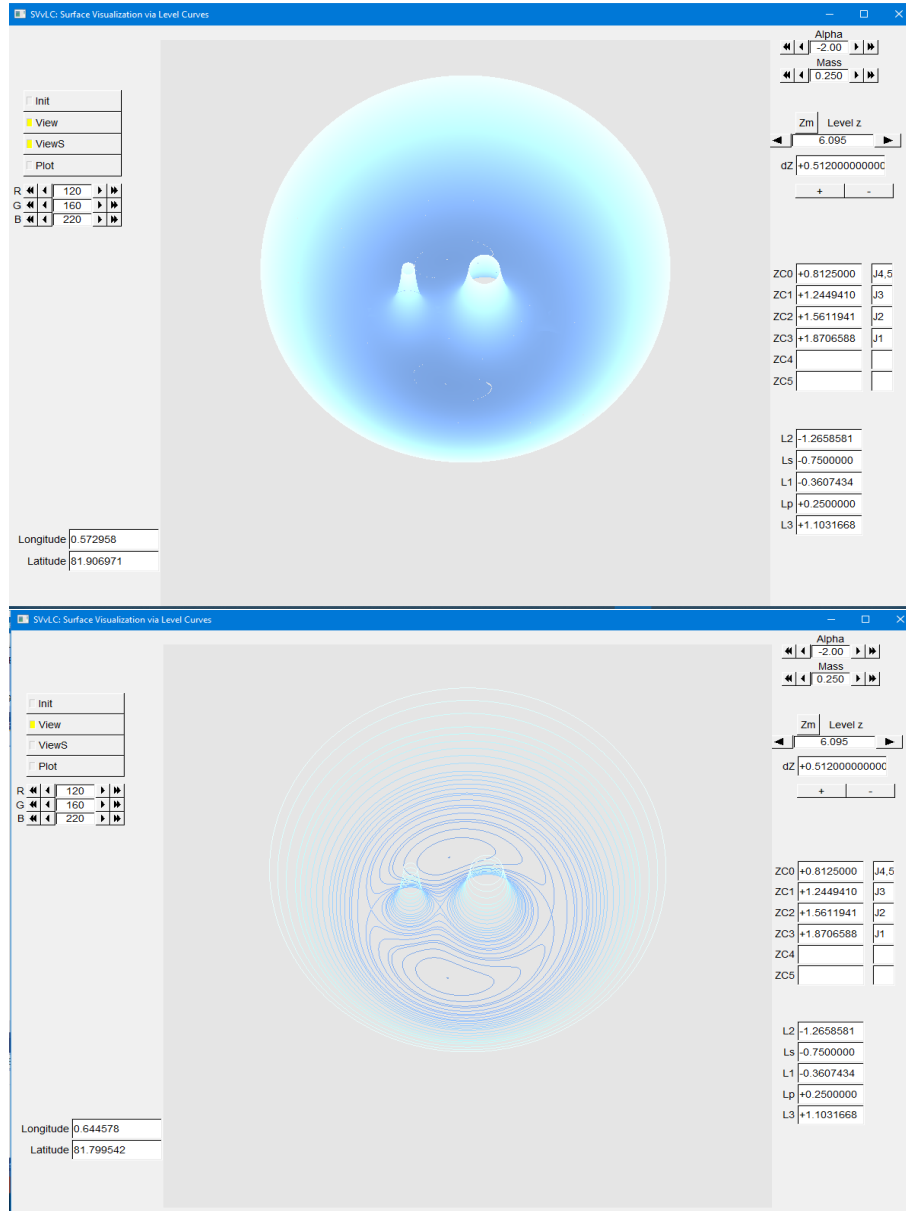


Figure B.2: Zero-velocity surfaces for $m = 0.25$, $\alpha = -2$.

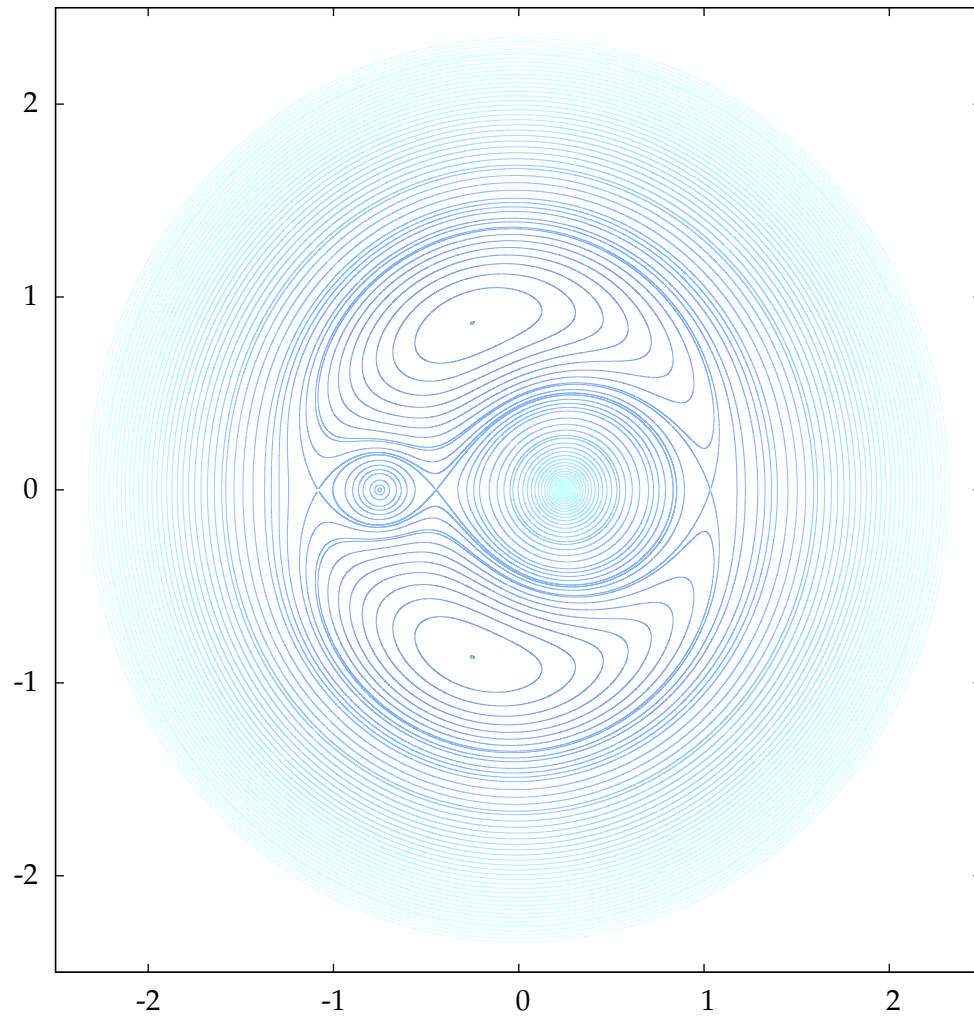


Figure B.3: Zero-velocity curves for $m = 0.25$, $\alpha = -0.50$.

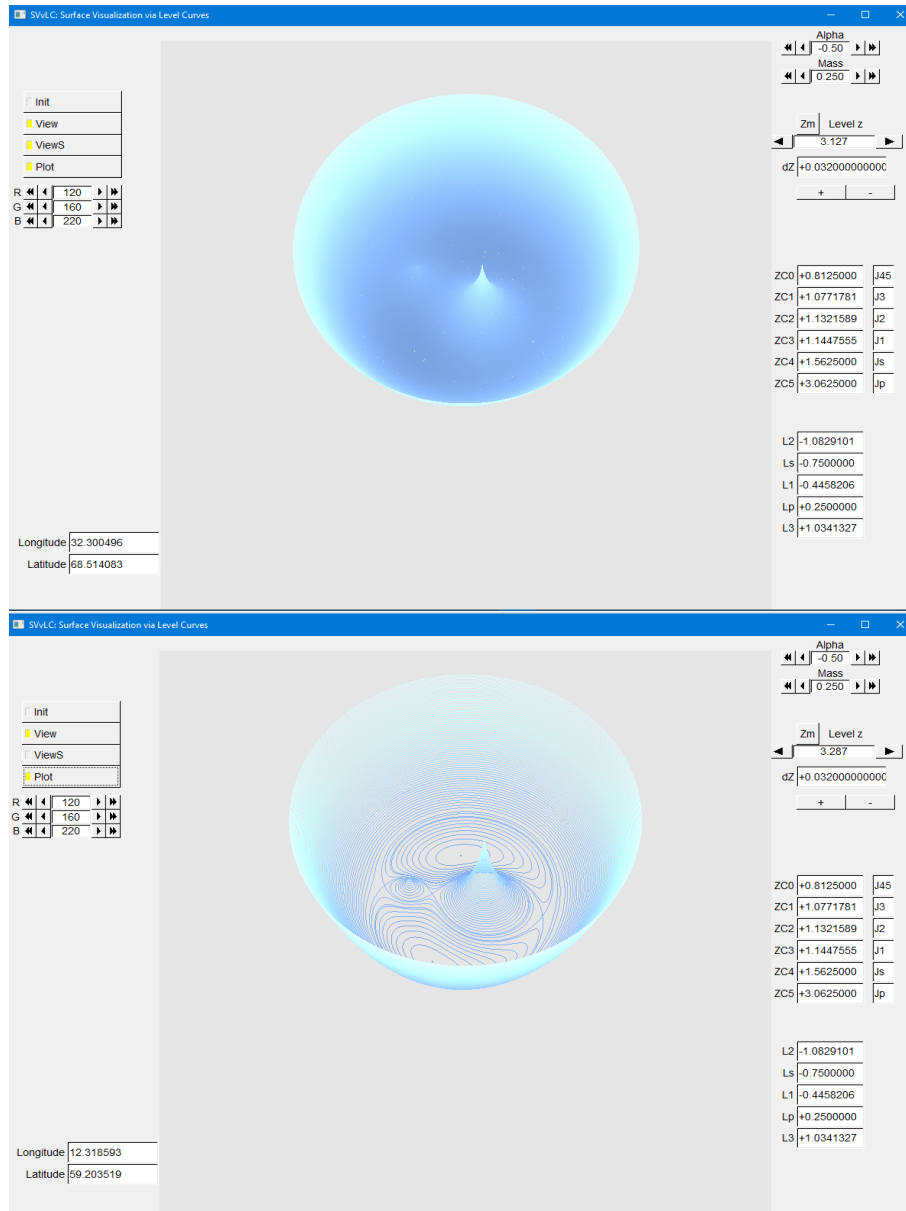


Figure B.4: Zero-velocity surfaces for $m = 0.25$, $\alpha = -0.50$.

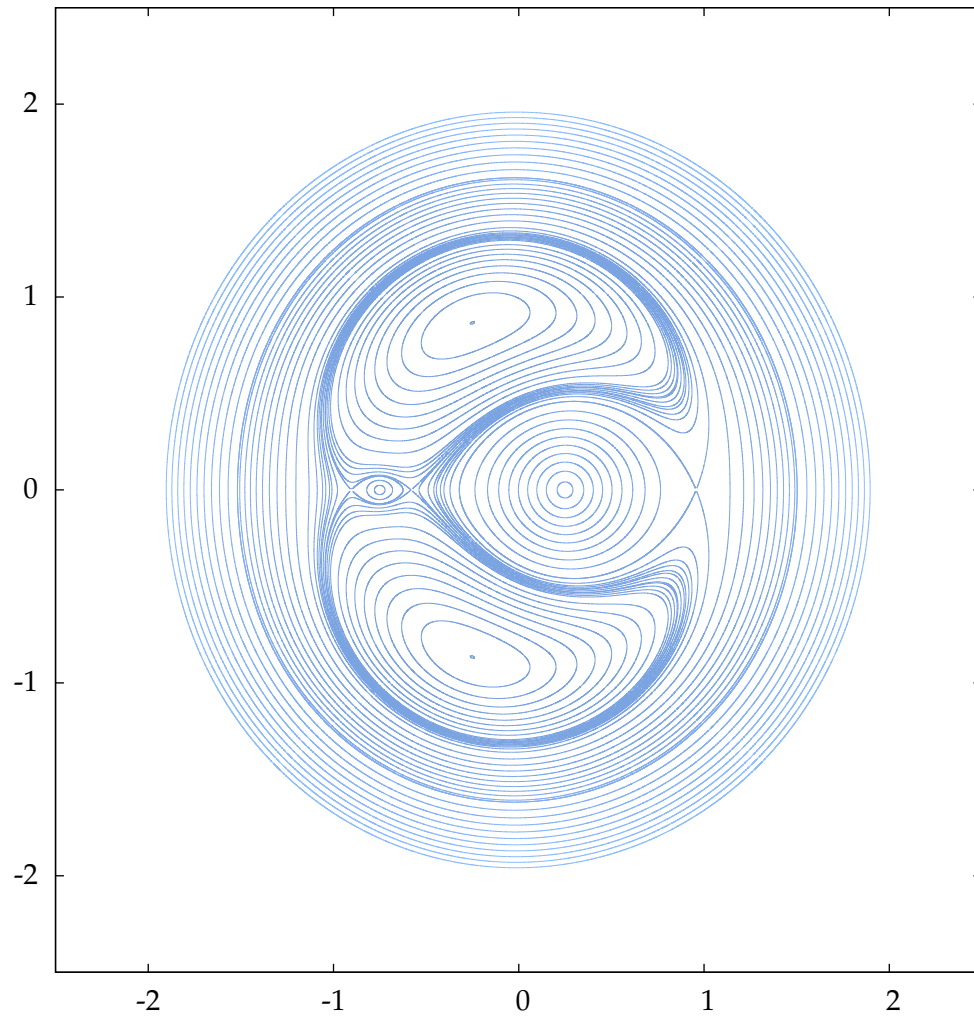


Figure B.5: Zero-velocity curves for $m = 0.25$, $\alpha = 0.50$.

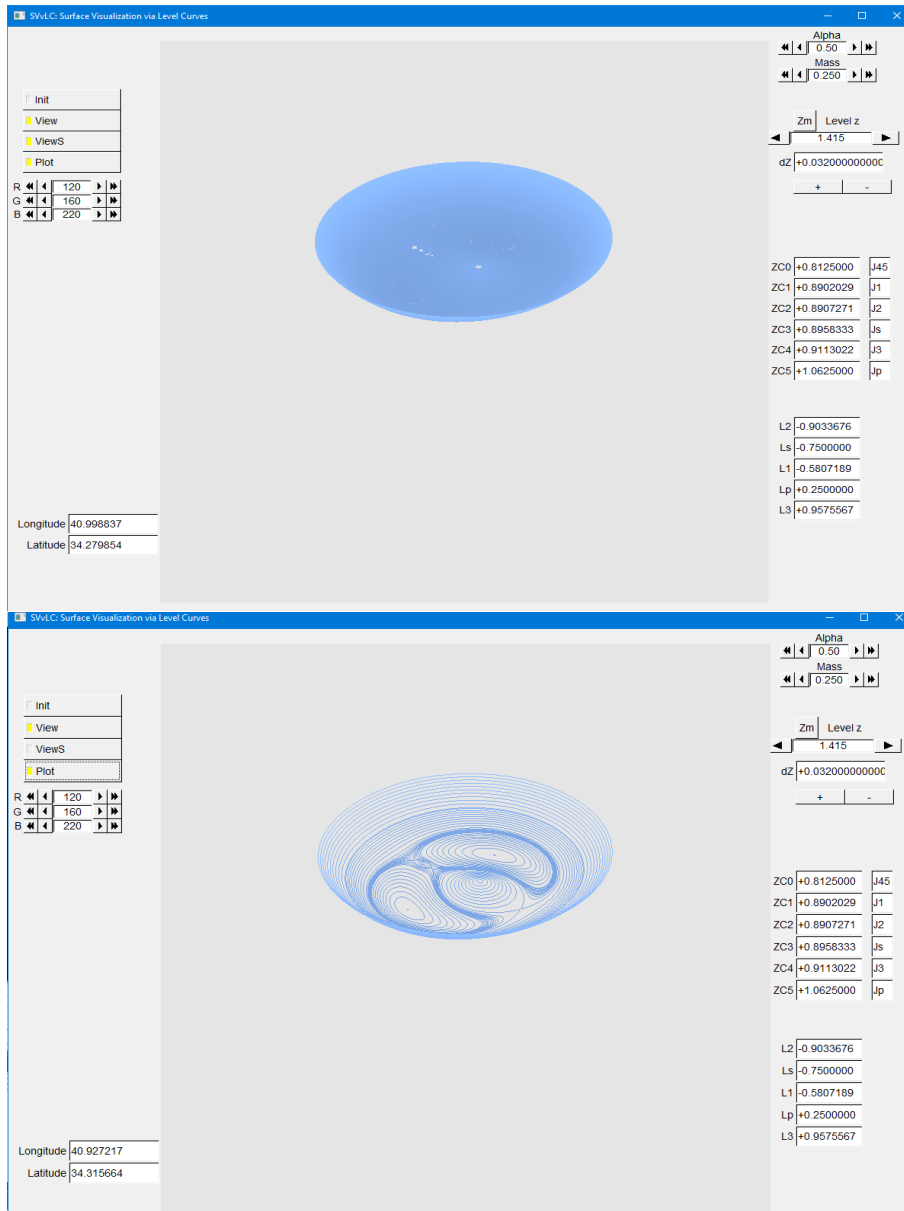


Figure B.6: Zero-velocity surfaces for $m = 0.25$, $\alpha = 0.50$.

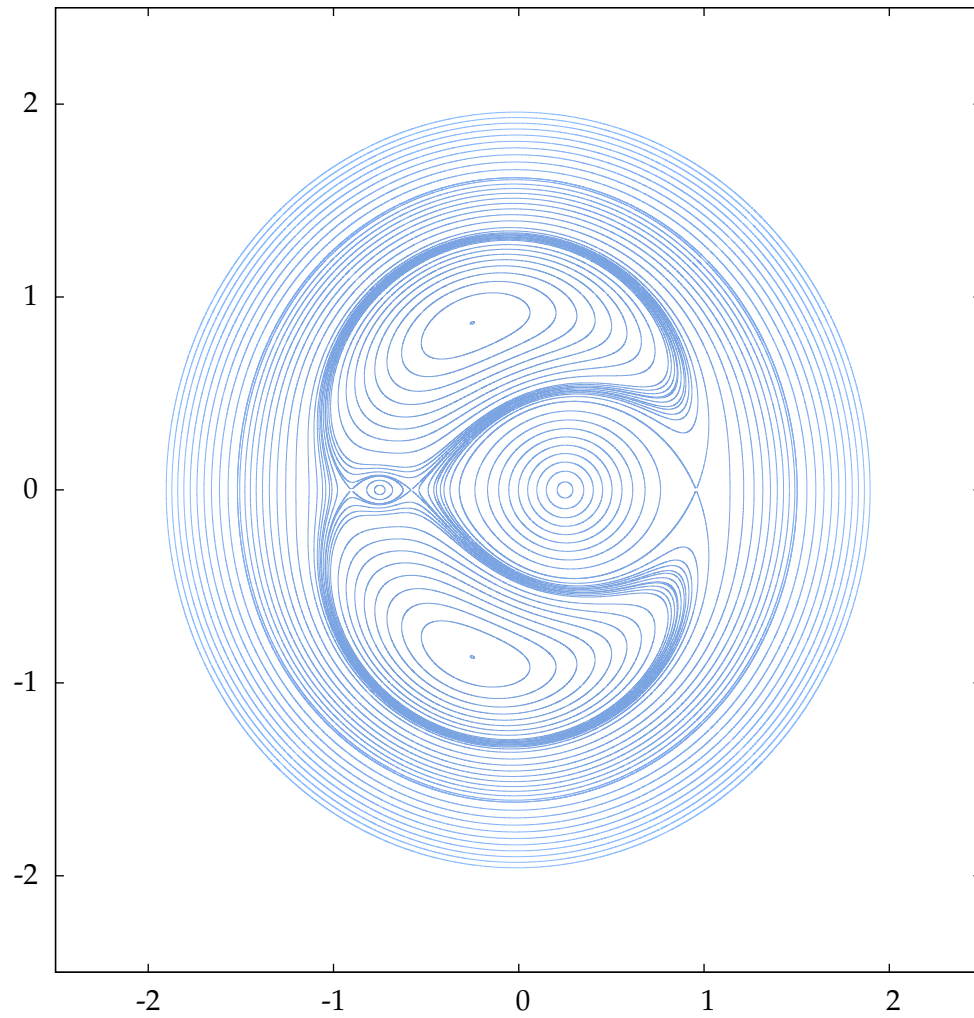


Figure B.7: Zero-velocity curves for $m = 0.25$, $\alpha = 1.50$.

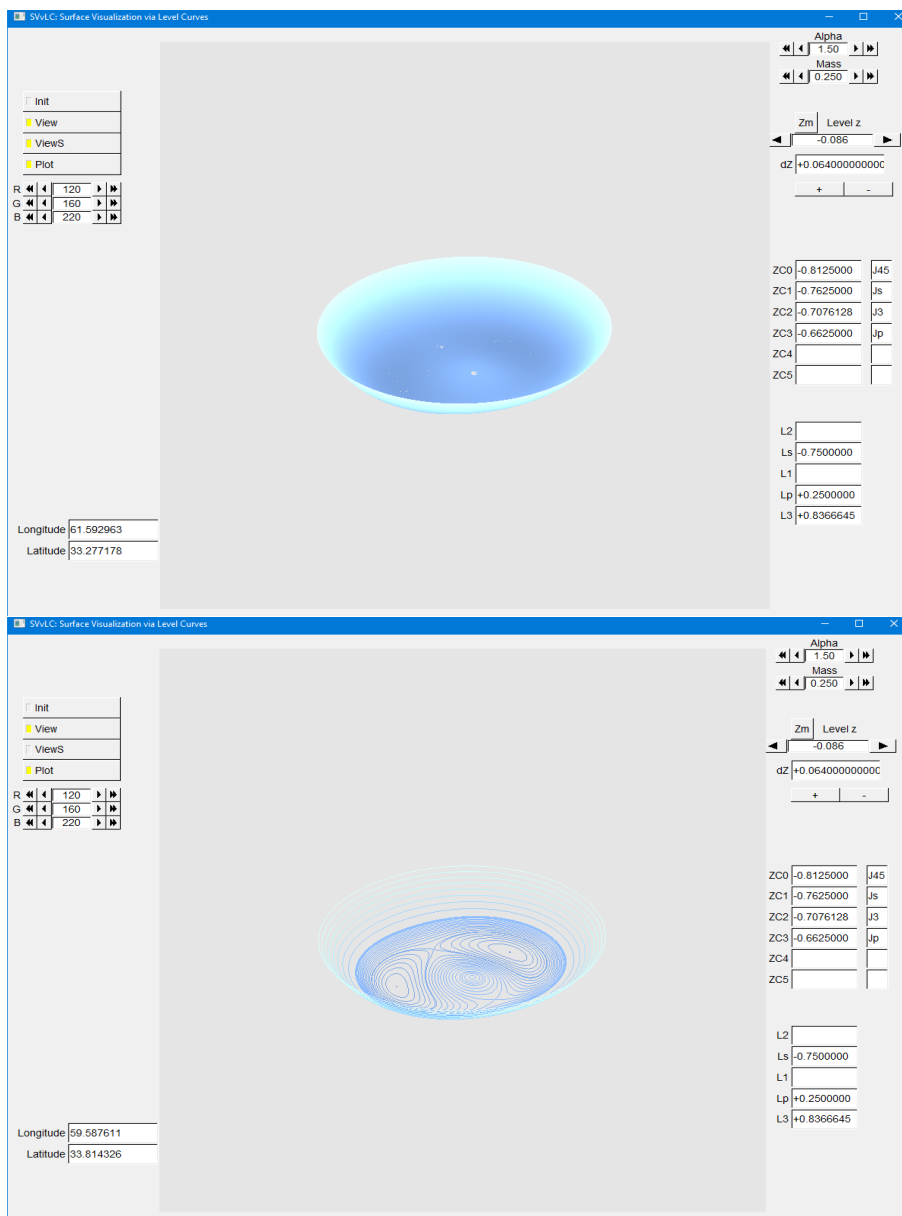


Figure B.8: Zero-velocity surfaces for $m = 0.25$, $\alpha = 1.50$.

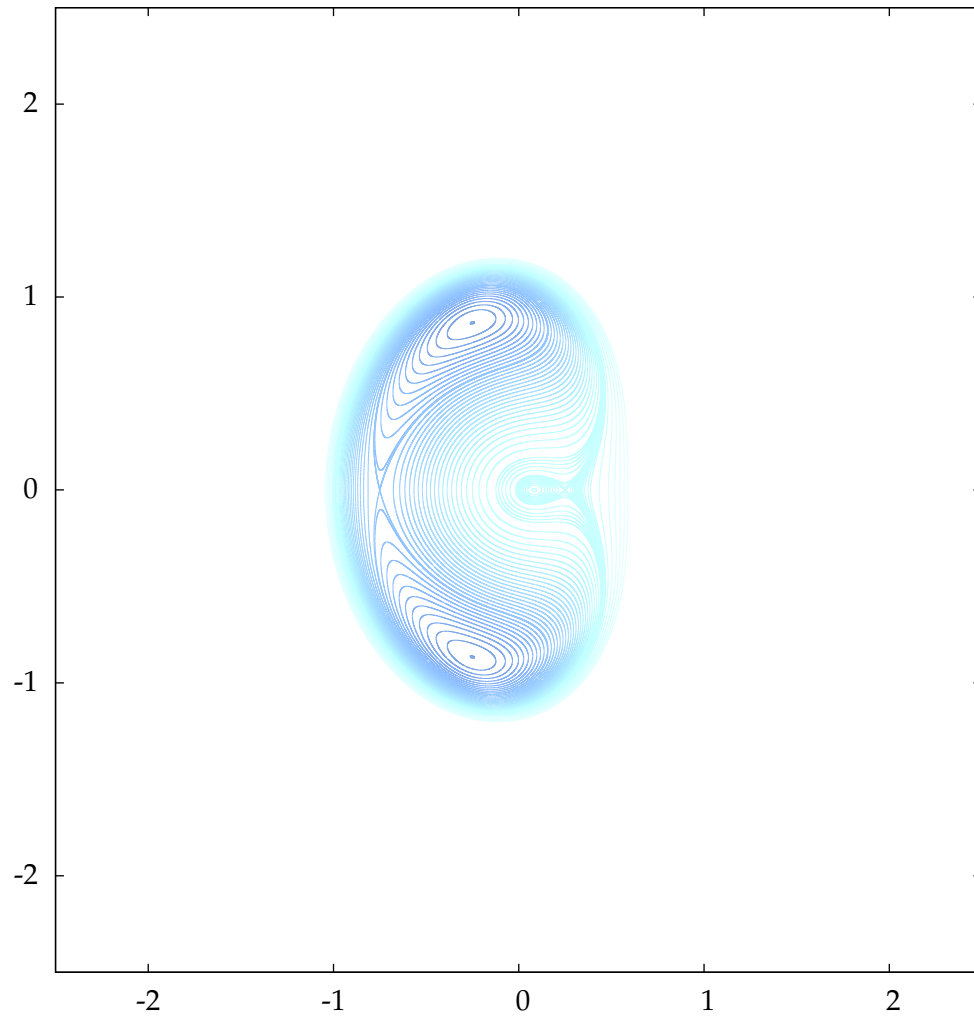


Figure B.9: Zero-velocity curves for $m = 0.25$, $\alpha = 6$.

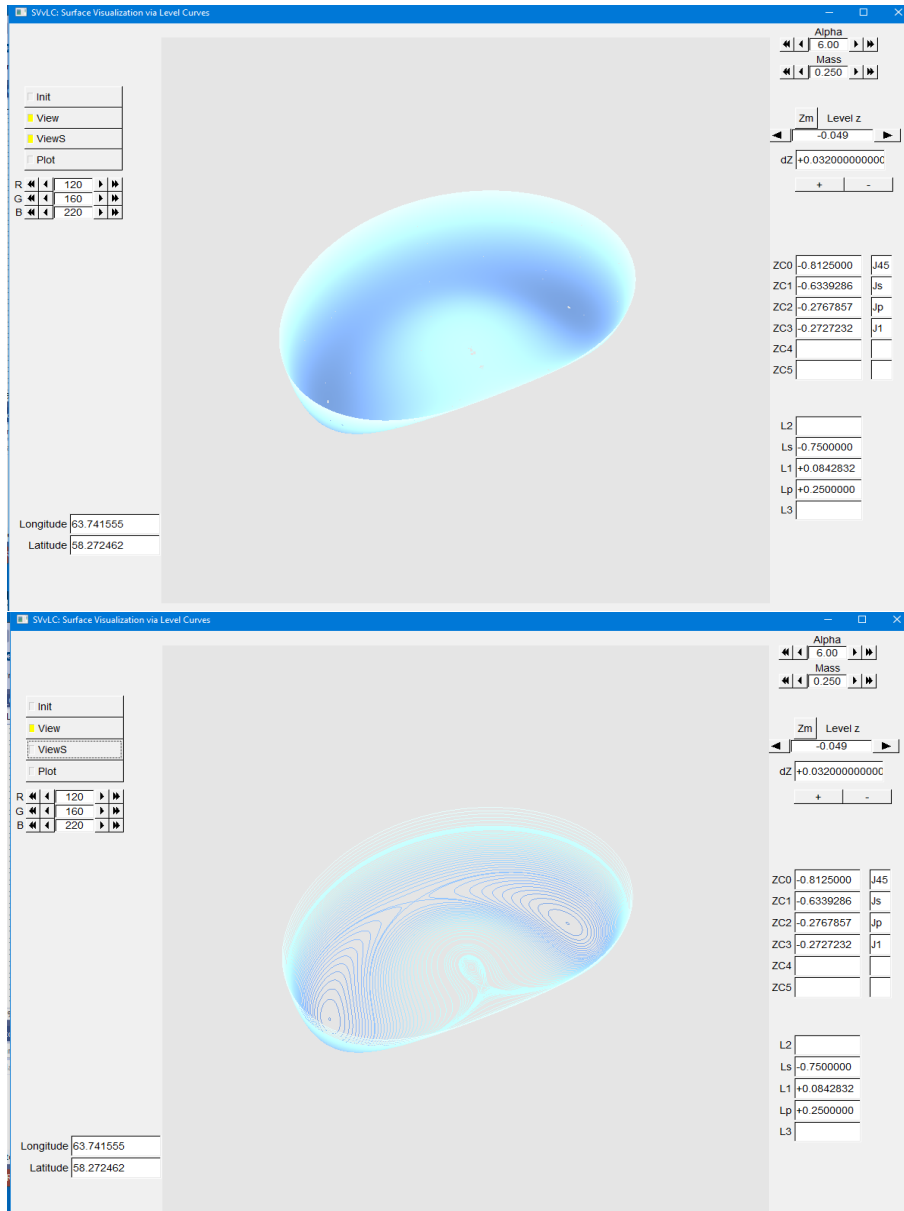


Figure B.10: Zero-velocity surfaces for $m = 0.25$, $\alpha = 6$.

Bibliography

- [1] H. Goldstein, *Mecánica Clásica*, Ediciones Aguilar, S.A., Madrid (1970).
- [2] V. G. Szebehely, *Theory of Orbits*, New York Academic Press (1967).
- [3] M. J. Valtonen, H. Karttunen, *The Three-Body Problem*, Cambridge University Press (2005).
- [4] R. L. Burden, J. D. Faires, *Numerical Analysis*, 9th edition, Brooks Cole (2011).
- [5] R. Symon, *Mechanics*, 3rd edition, Addison-Wesley Publishing Company (1971).
- [6] R. S. Wright, M. Sweet *Programación en OpenGL*, Anaya Multimedia (1997).
- [7] P. Holmes, E. T. Shea-Brown, *Stability*, www.scholarpedia.org, 15 Nov. 2013. Web.
- [8] E. Lopez Alonso *Problema de tres cuerpos restringido y circular*, Universitat de Barcelona (2020).

